# Engineering a Functionalized Biofilm-Based Material for Modulating Escherichia Coli's Effects in the Mammalian Gastrointestinal Tract

# Engineering a Functionalized Biofilm-Based Material for Modulating *Escherichia Coli's* Effects in the Mammalian Gastrointestinal Tract

Trevor R. Nash

A Thesis Presented to the
Commitee on Undergraduate Studies in Biomedical Engineering
in the
School of Engineering and Applied Sciences

in Partial Fulfillment of the Requirements
for the Degree with Honors
of Bachelor of Arts

Harvard University
Cambridge, Massachusetts

April 1, 2015

**Abstract**

This study investigates the potential use of engineered bacterial biofilms as programmable platforms to control bacterial-epithelial interactions in the mammalian gut. It is clear that commensal microflora play a critical role in the healthy functioning of the gastrointestinal tract, so this work seeks to use engineered biofilms to enhance and direct the therapeutic effects of such microbes. It is hypothesized that *E. coli* strains can be engineered to produce biofilm-based materials functionalized with peptides that will enhance colonization and modulate localized adhesion in the gut, while providing direct therapeutic effects themselves. A library of peptides has been identified, including the trefoil factor family peptides, as strong candidates for biofilm functionalization and *E. coli* have been successfully engineered to display these peptides on curli fibers that compose the extracellular biofilm. *In vitro* studies with epithelial cell cultures have demonstrated that *E. coli* secreting these modified curli fibers have enhanced epithelial adhesion, representing a strong starting point for the development of the desired programmable platform. Such a programmable platform has numerous potential downstream applications, such as producing and immobilizing therapeutic peptides and targeting specific inflammation sites, which could positively affect the treatment of inflammatory bowel diseases, such as ulcerative colitis and Crohn's disease, which affect more than 1.4 million Americans.

# Contents

# List of Figures

# List of Tables

# 1 Introduction

## 1.1 Significance of Work

Reported cases of inflammatory bowel diseases (IBD), including Crohn's disease and ulcerative colitis, have increased significantly in recent decades, with over 1.4 million Americans suffering from these conditions today (CDC, 2014). These diseases have numerous deleterious symptoms, such as persistent diarrhea, perforated bowels, and rectal bleeding, that can drastically reduce the patient's quality of life (Fakhoury et al., 2014). These are chronic diseases with no known cure, so current therapies seek to reduce symptoms through the administration of NSAIDs, corticosteroids, immunomodulators, and antibiotics. Such therapies are not permanent solutions, and they are not effective for many patients, so there is a great need for the development of more potent IBD treatments.

With a rapidly growing body of literature reporting the critical role that the gastrointestinal microbiome plays in the maintenance of human health (Consortium, 2012), there is an increasing interest in the clinical use of orally administered bacteria for the treatment of various conditions, including IBD. Naturally derived strains of probiotic bacteria are already used around the world, and researchers have begun to investigate the use of artificially engineered bacteria for the delivery of therapeutics. Studies have reported the successful engineering of commensal bacterial strains to secrete recombinant cytokines and other biologics that have reduced symptoms of IBD in mouse models (Steidler et al., 2003; Steidler et al., 2006; Vandenbroucke et al., 2004). While such successes are promising, these methods have no way of targeting or localizing this therapy to specific regions of the gastrointestinal tract. Therefore, this current work presents the initial steps towards the development of a system in which commensal bacteria are engineered to secrete and assemble biofilm-based materials

functionalized with peptides that will enhance colonization and modulate localized adhesion of the expressing bacteria in the gut, while providing direct therapeutic effects itself.

## 1.2 Hypothesis

As a starting point for the development of the platform described above, this work hypothesizes that *E. coli* strains can be engineered to produce biofilms displaying functional peptides that will increase the *in vitro* adhesion of the expressing bacteria to human gastrointestinal epithelial cells while maintaining the biological activity of these displayed peptides.

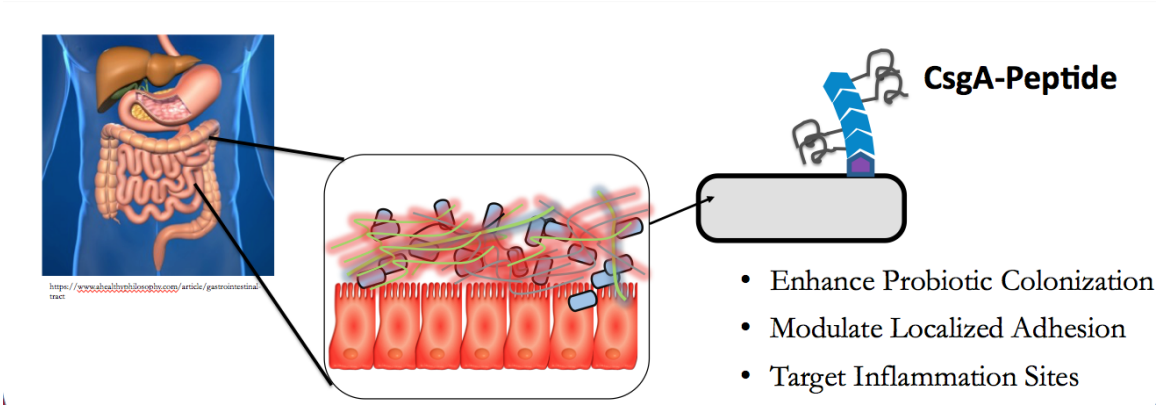


Figure 1: Overview of the proposed biofilm-based platform and its applications. CsgA refers to the protein monomer building block of *E. coli* biofilms.

## 1.3 Specific Aims

To test this hypothesis, research was guided by the following specific aims:

1. Identify a selection of functional peptides for biofilm display and genetically engineer a library of plasmids encoding curli fibers modified with these peptides in different arrangements.

2. Transform the library plasmids into *E. coli* and confirm that these transformants successfully express curli fibers properly displaying the desired functional peptides.

3. Assess the effects of the functionalized curli fiber library members on the *in vitro* adhesion of transformed *E. coli* to human gastrointestinal epithelial cells.

4. Determine whether the curli-displayed peptides retain their normal biological activity.

# 2 Background and Literature Review

## 2.1 Biofilms & Curli Fibers

Although bacterial biofilms are often associated with negative connotations and thought of as nuisances that should be destroyed, this work seeks to build on a growing trend of research trying to productively use biofilms for a variety of applications. One such approach, which this work will employ, relies on the modification of biofilms by genetically engineering the bacteria that secrete them (Nguyen et al., 2014). To engineer biofilms in such a way, their fibrous subunits that weave together into the biofilm mesh must be modified at the monomer level. These fibers of interest are curli fibers, the major proteinaceous component of *E. coli* biofilms, and they are polymers assembled from CsgA protein monomers.

Curli fibers are amyloid nanofibers expressed on the surface of Enterobacteriaceae, a large family of Gram-negative rod-shaped bacteria, including the commensal *E. coli* strains that inhabit the human gut microbiome (Chapman et al., 2002). Unlike the pathogenic amyloids in human cells that are the result of misfolded proteins and contribute to numerous deleterious conditions, including Alzheimer's and Huntington's diseases, curli fibers are produced by a dedicated biosynthetic pathway in Enterobacteriacae, known as the nucleation-precipitation secretion pathway (Barnhart & Chapman, 2006). Before attempting to engineer these fibers and use this natural self-assembly mechanism for novel, non-natural applications, a strong working knowledge of this pathway and its components is required.

### 2.1.1 Curli Biogenesis Pathway

Involving six proteins encoded on two different divergently transcribed operons (*csgCBA* and *csgDEFG*), the bacterial nucleation-precipitation pathway allows the se-

cretion of the amyloidogenic protein CsgA and then the extracellular self-assembly of these CsgA subunits into networks of fibers to create a biofilm (Hammar et al., 1995; Chapman et al., 2002; Gerven et al., 2014). The *csgCBA* operon encodes this CsgA protein, the 13-kDa primary structural component of curli fibers, along with CsgB, a nucleator protein that assembles CsgA polymers and anchors these assembled nanofibes to the bacterial cell surface (Nguyen et al., 2014). Experiments have shown that soluble CsgA monomers are secreted from the cell and then assembled extracellularly by CsgB proteins that can originate from the same cell as the CsgA or from different bacterial cells, so this assembly is classified as interbacterial complementation and allows the creation of dense networks of tangled curli fibers surrounding large numbers of bacterial cells (Hammar et al., 1996). CsgC is the third gene in this operon, but its specific function in curli biogenesis has yet to be elucidated (Barnhart & Chapman, 2006). Its transcripts were only recently discovered during curli production, and subsequent studies have suggested that CsgC has some redox activity, with the transmembrane transporter CsgG being a likely target for regulation of the secretion of CsgA and CsgB (Taylor et al., 2011). An even more recent study suggests that CsgC may in fact inhibit amyloid formation and may be used as a negative regulator of the curli biogenesis pathway, but more research must be conducted to further confirm this hypothesis and to determine the effects of modulating CsgC on the curli biogenesis pathway as a whole (Evans et al., 2015).

The four proteins encoded by the *csgDEFG* operon are accessory proteins necessary for curli assembly that contribute to the regulation of *csgCBA* transcription and carry out the post-translational processing and secretion of CsgA and CsgB (Barnhart & Chapman, 2006). CsgD is a positive transcriptional regulator of the *csgCBA* operon that likely binds the *csgCBA* promoter, as it is required for CsgA and CsgB transcription (Hammar et al., 1995). CsgD not only regulates curli assembly, but it

also plays an important role in the production of cellulose, the other major component of the *E. coli* extracelluar matrix, as it activates *adrA*, which is required for the production of cellulose (Zogaj et al., 2001; Simm et al., 2004). CsgG is an oligomeric transporter lipoprotein in the bacterial outer membrane. Recent structural studies have shown that it consists of a "cage-like vestibule" in the periplasm connected to a 36-stranded $\beta$-barrel with an approximately 2 nm diameter pore that extends through the phospholipid bilayer of the outer membrane (Goyal et al., 2014; Taylor et al., 2011). This channel is thought to be ungated and reliant on a diffusion-based and entropy-driven transport mechanism (Goyal et al., 2014). Despite this apparent non-specificity, studies have shown that the N-terminal 22 amino acids of CsgA are required for its secretion through CsgG, but the details of this mechanism have yet to be elucidated (Robinson et al., 2006). CsgE and CsgF are both soluble periplasmic proteins that physically interact with CsgG at the outer membrane, but the specifics of these molecular interactions are currently unknown. *E. coli* strains without *csgE* or *csgF* cannot effectively produce curli, but these different deletion strains have distinct phenotypes (Barnhart & Chapman, 2006). *CsgE* deletion strains produce unstable CsgA and CsgB proteins and can only assemble very few curli fibers that are morphologically distinct form wild type curli fibers, while *csgF* deletion strains do not assemble curli fibers, only secreting soluble, unpolymerized CsgA (Chapman et al., 2002). Further studies are needed to determine the specifics of the molecular mechanisms underlying these phenotypes.

### 2.1.2 Physical Characterization of Curli Fibers

Curli fibers are classified as amyloids due to the many biochemical and physical properties that they share with eukaryotic fibers. They are nonbranching (Chapman et al., 2002) and have the conserved cross $\beta$-strand structure that characterizes amyloid

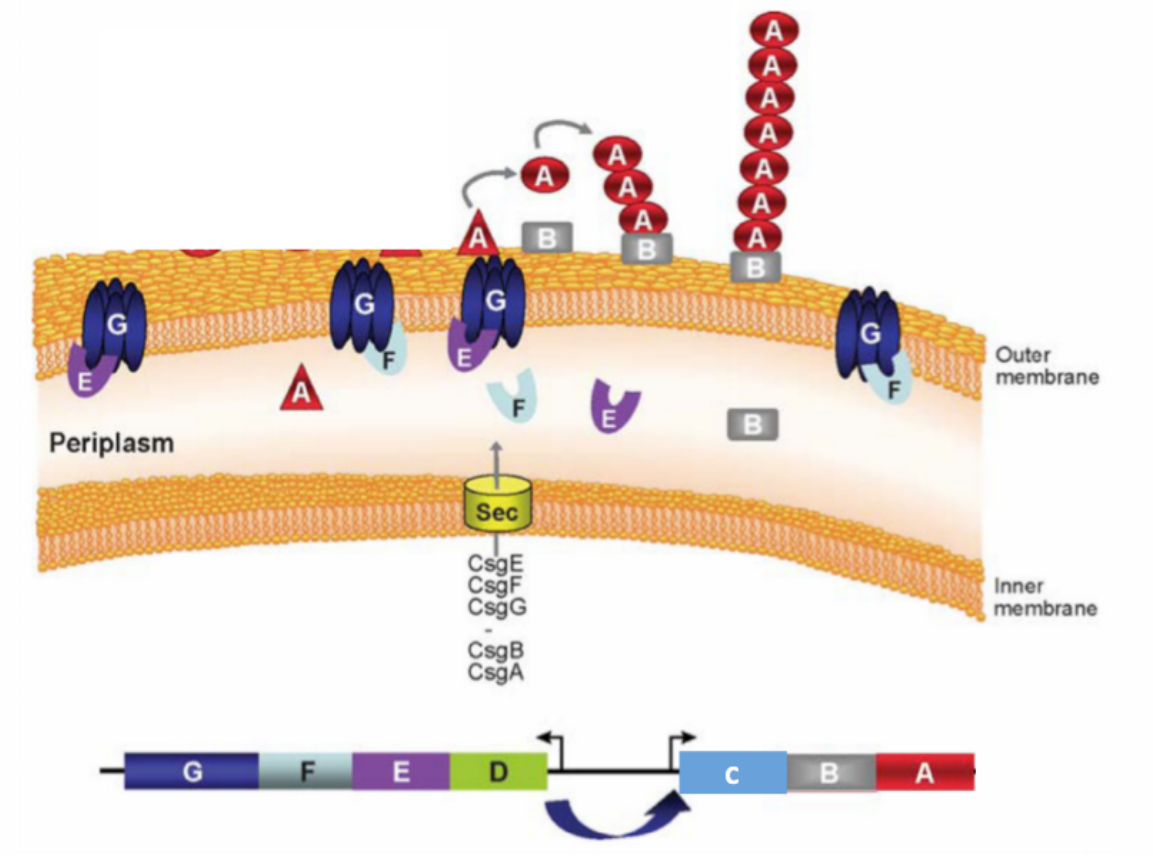


Figure 2: Curli biogenesis pathway, adapated from Figure 1 of Barnhart & Chapman, 2006.

fibers (Barnhart & Chapman, 2006; Sunde & Blake, 1997). In this structure, $\beta$-sheets are stacked parallel to the length of the fiber, with individual $\beta$-strands perpendicular to this axis. Based on computer models, CsgA is predicted to have five repeating strand-loop-strand motifs of $\beta$-strands that form $\beta$-sheets in each monomer of curli fibers. The repeating $\beta$-strand motifs form rings, giving curli fibers a cylindrical morphology with diameters between approximately 4 and 7 nm (Nguyen et al., 2014). Each of these $\beta$-strand motifs contains conserved glycine, glutamine, and asparagine residues, which are also found in many eukaryotic amyloid fibers (Michelitsch et al., 2000). It is though that many of these glutamine and asparagine residues form hydrogen bonds that contribute to the stability, robustness, and strength of amyloid

fibers (Perutz et al., 2002).

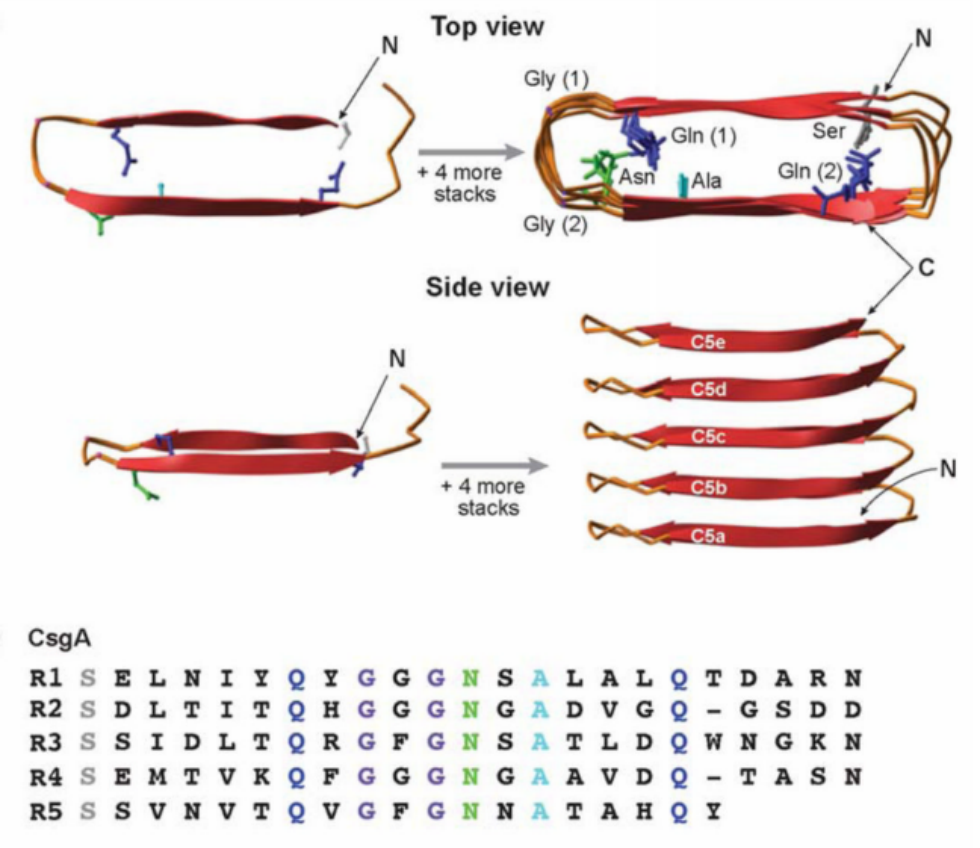


Figure 3: Model of CsgA structure based on the predicted strand-loop-strand motif. Each of the five listed repeating units (R1-R5) is one strand-loop-strand. Reproduced from Figure 6 of Barnhart & Chapman, 2006.

Due to their $\beta$-sheet amyloid structure, curli fibers are highly resistant to both chemical degradation and proteolysis (Collinson et al., 1991). They have been shown to be resistant to digestion by proteases and 1% sodium dodecyl sulfate (Collinson et al., 1993), and they have even been shown to withstand boiling in detergents and extended incubation in various solvents (Hammar et al., 1995), making them very robust for applications in harsh environments and able to be readily purified from the rest of the components of the cellular and extracellular milieu that would be degraded under such conditions. Although such mechanical characterization of curli has yet to

be conducted, studies of amyloid fibers similar to curli fibers have shown that these fibers have strength comparable to steel, yet mechanical stiffness equivalent to that of silk (Smith et al., 2006).

Like all amyloids, curli fibers experience a red shift with an increase in their emission wavelengths when mixed with the amyloid-staining diazo dye Congo red (Klunk et al., 1999), and this Congo red dye can be used as an effective indicator of curli fiber expression and proper assembly in *E. coli* (Collinson et al., 1993). Curli fibers also trigger a 10 to 20 fold increase in fluorescence in the presence of thioflavin T (Chapman et al., 2002), which is another defining characteristic of amyloid fibers (LeVine, 1999).

Although it was originally thought that amyloids are only formed through accidental protein misfolding in eukaryotes, other functional amyloids have recently been discovered in a wide variety of species, including yeast, fungi, and mammals, indicating that curli fibers are not a biological anomaly (Barnhart & Chapman, 2006).

### 2.1.3 Physiological Function of Curli Fibers

As functional amyloids, curli fibers serve a variety of functions in both pathogenic and symbiotic bacteria. Generally expressed under stressful conditions, they are critical for the formation of biofilms, the enhancement of adhesion to the intestinal mucosa, and the modulation of invasiveness in pathogenic strains (Koli et al., 2011).

## 2.2 The Biofilm-Integrated Nanofiber Display (BIND) System

Previously published work has successfully engineered the curli biogenesis pathway to display desired peptides on curli fibers using a system called BIND. There are

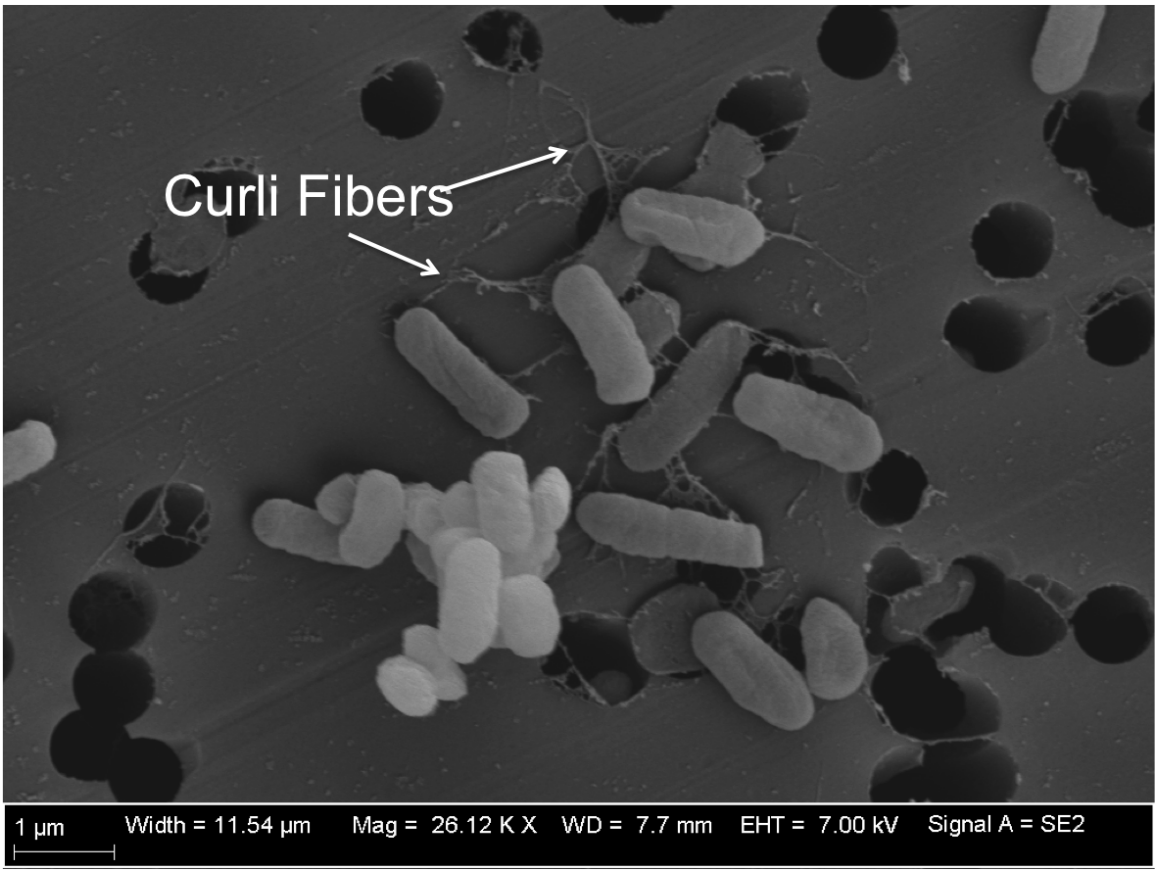


Figure 4: SEM Image of *E. coli* cells expressing unmodified wild type curli fibers. A scale bar is shown in the bottom left of the image; 26,120x magnification.

numerous advantages to harnessing curli fibers and their biogenesis as a platform for synthetic biology, including the self assembly of CsgA monomers into curli fibers, the robustness of curli fibers, and the demonstrated ability of the curli mechanism to export natively unfolded polypeptides attached to curli fibers (Gerven et al., 2014).

The native curli mechanism can be harnessed to create a programmable, functionalized biofilm that displays non-native peptides by appending functional peptide domains to the C-terminus of the *csgA* gene. These chimeric CsgA variants are secreted and assembled by the cell's natural export machinery, yielding biofilms that structurally resemble wild-type curli biofilms but have the functionality of the fused

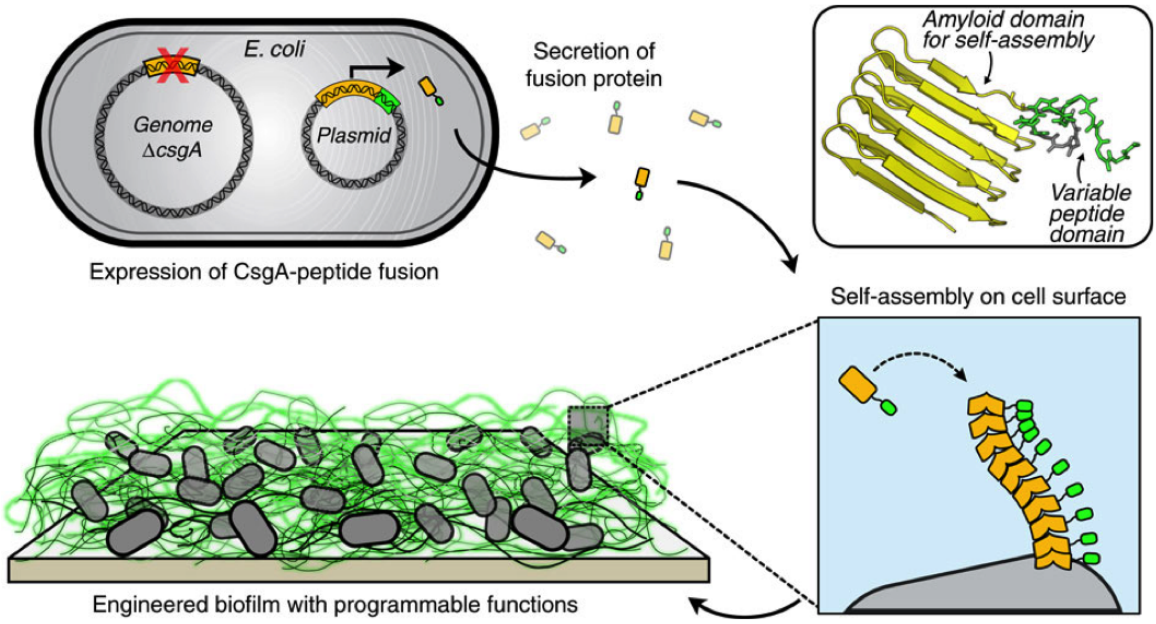


Figure 5: Overview of the BIND system. Reproduced from Figure 1 of Nguyen et al., 2014.

peptide (Nguyen et al., 2014). The other genes in the *csgCBA* and *csgDEFG* operons are not deleted and are expressed under native control. The engineered *csgA* fusion gene, however, is under control of an IPTG-inducible promoter on the engineered plasmid and will be over expressed in the presence of IPTG.

## 2.3 Trefoil Factor Family Peptides

The trefoil factor family is a class of three peptides (TFF1,TFF2,TFF3) that have been shown to be important for the protection and repair of the gastrointestinal epithelium (Playford et al., 1995). They all have at least one characteristic conserved P domain, which contains a trefoil triple loop structure formed by three cysteine-cysteine disulfide bridges (Thim, 1997). The signaling mechanisms of the peptides have yet to be elucidated, but they are known to affect barrier function, gene transcription, and cell migration. All three peptides are upregulated in patients with

ulcerative colitis or Crohn's disease (Wright et al., 1990; Podolsky, 1997; Poulsom et al, 1993), leading to the hope that these peptides could be used therapeutically for the treatment of these inflammatory bowel conditions. Recombinant TFF peptides are currently under investigation in multiple clinical trials for the treatment of IBD (Hoffmann, 2009; Aamann, 2014), but peptide delivery will likely remain problematic due to the difficulty of transporting peptides through the stomach without significant degradation. Accordingly, the use of engineered probiotic *Lactococcus lactis* has been investigated for the *in vivo* delivery of recombinant TFF3 in the intestine with promising results in mouse models (Vandenbroucke et al.,2004), but such a therapy has yet to undergo any human clinical trials.

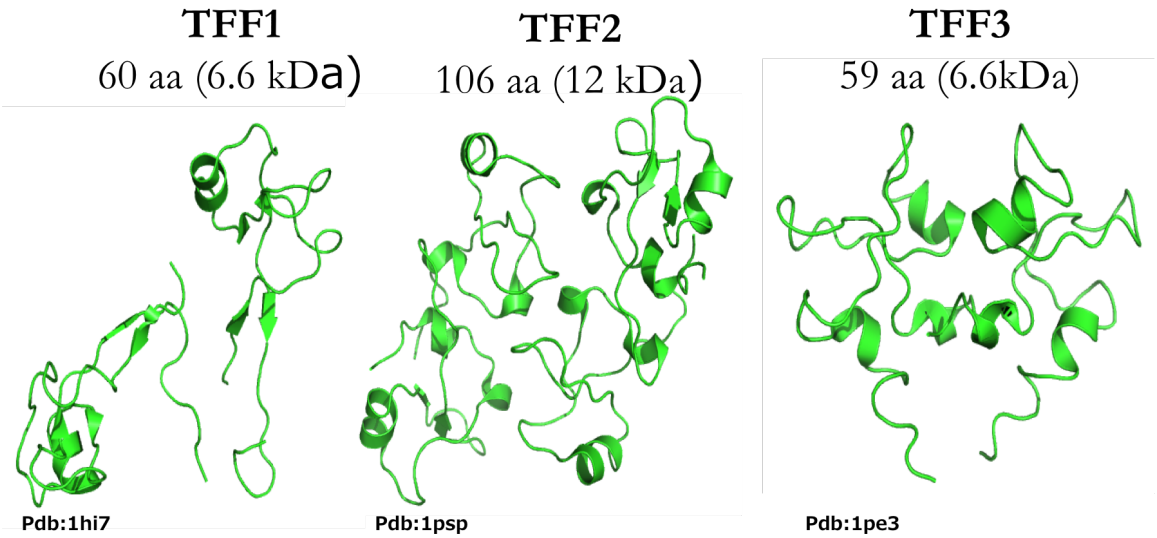


Figure 6: Trefoil factor family peptide 3D structures.

## 2.4 Synthetic Peptides with Affinity for the Intestinal Epithelium

Numerous previous studies have used phage display with large libraries of short synthetic peptides to determine which peptides, if any, have affinity for different epithelial

cell types within the gastrointestinal tract. These studies have identified the so called A1 and CP15 synthetic peptides as having affinity for colon carcinomas (Costantini, et al., 2009; Zhang et al., 2007), the P8 peptide as having affinity for M cells in the follicle-associated epithelium (Higgins et al., 2004), and the T18 peptide as having affinity for injured epithelial cells (Hsiung, et al.,2008). Due to such specific binding affinities, these peptides are excellent candidates for biofilm display for the purposes of this study.

# 3 Genetic Engineering of Functionalized Curli Fibers

## 3.1 Overview of Functional Peptides

Building off the previously described BIND system for the display of functional peptides on curli fibers in bacterial biofilms (Nguyen et al., 2014), this study sought to display peptides that would likely interact with the endothelium of the mammalian gastrointestinal tract to influence the adhesion of the displaying bacteria and/or modulate natural physiological processes of the host endothelial cells. The three peptides from the trefoil factor family (TFF1, TFF2, and TFF3) were chosen for their natural expression at various locations within the human gastrointestinal tract and their known effects on various physiological and therapeutic pathways in gastric epithelial cells (Taupin & Podolsky, 2003). It should be noted that TFF3 has a three-loop tertiary structure involving three cysteine-cysteine disulfide bridges (Thim, 1997; Figure 7) that may pose a challenge to the curli secretion machinery. Therefore, truncated versions of the TFF3 peptide with the individual loops and combinations of the loops were also engineered to be displayed on curli fibers to determine the effect of this tertiary structure on modified curli secretion and assembly. Additionally, these variants will provide insight into the functional domains of the TFF3 peptide, as the biological functionality of these truncated versions will be compared with that of the full peptide. Four short synthetic peptides (A1, CP15, P8, and T18) were also chosen that previous studies had screened for their affinity for specific types of cells within the human gastrointestinal tract. The amino acid sequences of these peptides are shown in Table 1.

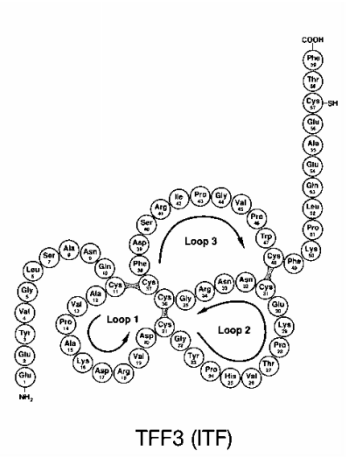


Figure 7: TFF3 Loop Structure.

## 3.2 Design of Engineered Genetic Vectors

To use the BIND system and hijack the *E. coli's* native curli biogenesis machinery through the nucleation-precipitation pathway, the DNA sequences encoding the desired functional peptides must be added to the *csgA* gene. This way, the native cellular transcription machinery will not only transcribe *csgA*, but will continue to produce a single mRNA strand encoding both CsgA and the functional peptide. This mRNA will then be processed by native ribosomes to produce CsgA curli subunits fused to the desired functional peptide. Previous work with the BIND system has demonstrated that the optimal location for the addition of the functional peptides is at the C-terminal end of the *csgA* gene, but with the addition of a flexible "linker" region between *csgA* and the peptide sequence (Nguyen et al., 2014). When translated, this linker will connect the functional peptide to the CsgA monomer, but provide space between the two and flexibility that will likely influence the ability of the native machinery to secrete and assemble the fusion protein. Various linkers have been tested with the BIND system, with flexible linkers containing a repeating glycine-glycine-glycine-serine motif proving to be the most effective for secretion and

| **Peptide** | **Amino Acid Sequence** | **Localized Adhesion** |
|---|---|---|
| TFF1 | EAQTETCTVAPRERQNCGFPGVTPSQCANKGC CFDDTVRGVPWCFYPNTIDVPPEEECEF | Gastric Surface |
| TFF2 | EKPSPCQCSRLSPHNRTNCGFPGITSDQCFDNGCC FDSSVTGVPWCFHPLPKQESDQCVMEVSDRRN CGYPGISPEECASRKCCFSNFIFEVPWCFFPK SVEDCHY | Stomach |
| TFF3 | EEYVGLSANQCAVPAKDRVDCGYPHVTPKECNNR GCCFDSRIPGVPWCFKPLQEAECTF | Small and Large Intestines |
| A1 | VRPMPLQ | Colon Cancer Cells |
| CP15 | VHLGYAT | Colon Cancer Cells |
| P8 | LETTCASLCYPS | M Cells, Follicle-Associated Epithelium |
| T18 | LTHPQDSPPASA | Injured Epithelial Cells |

Table 1: Functional Peptides Investigated in this Study

assembly (Nguygen et al., 2014). For this study, linkers comprised of 12, 24, and 48 amino acid residues were used, containing 3, 6, and 12 repeats of this glycine-serine motif, respectively (Table 2).

Figure 8 provides an overview of the entire *csgA*-linker-functional peptide genetic engineering scheme. This figure also includes the significant regions of the *csgA* gene itself, including the periplasmic localization sequence, 22 amino acid CsgG-mediated secretion sequence, and the five repeating loop- $\beta$-strand-loop motifs that make up the structural $\beta$-sheets of CsgA. Table 3 lists all of the linker-peptide combinations that were developed and investigated in this study. For clarity, the nomenclature used for these constructs was CsgA-linker_length-functional_peptide. For example, TFF1

| Linker | Amino Acid Sequence |
|---|---|
| F12 | GGGSGGGSGGGS |
| F24 | GGGSGGGSGGGSGGGSGGGSGGGS |
| F48 | GGGSGGGSGGGSGGGSGGGSGGGSGGGSGGGSGGGSGGGS GGGSGGGS |

Table 2: Linkers Used in this Study

fused to CsgA with a 48 amino acid linker would be called CsgA-48-TFF1.

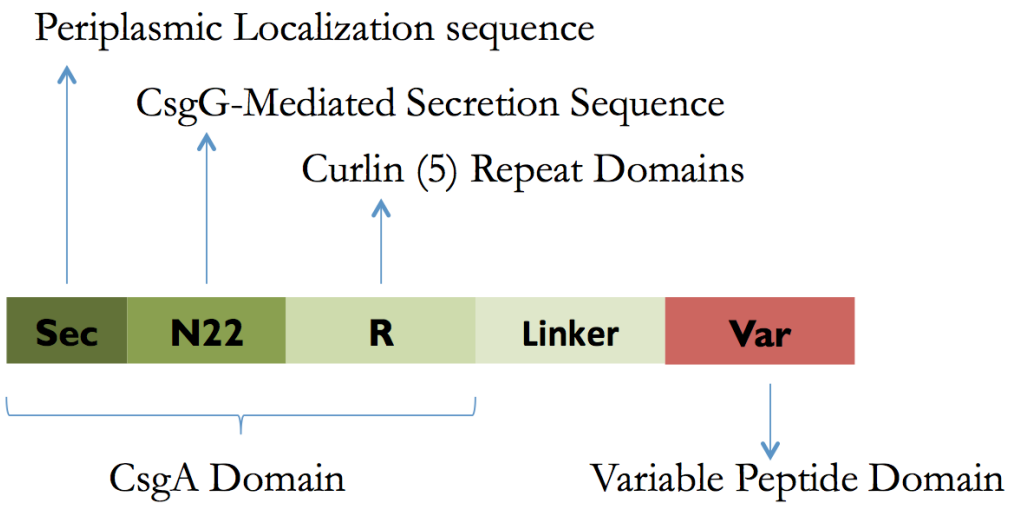


Figure 8: Overview of the CsgA Construct Architecture

For expression of these genetic constructs, they must be cloned into a plasmid that can be electroporated into competent host cells. For selection of cells into which the plasmid has been successfully transformed, this plasmid must also confer specific antibiotic resistance to its host. For this study, plasmids containing ampicillin resistance were used, enabling the use of ampicillin LB plates for the selection of transformed colonies. During downstream applications for curli production, ampicillin could also be added to growth media to ensure cells that dropped the engineered plasmid did not survive.

| Construct Library | |
|---|---|
| Trefoil Factor Family Peptides | CsgA-24-TFF1 |
| | CsgA-24-TFF2 |
| | CsgA-24-TFF3 |
| | CsgA-12-TFF3 |
| | CsgA-48-TFF1 |
| | CsgA-48-TFF2 |
| | CsgA-48-TFF3 |
| TFF3 Loops | CsgA-24-TFF3_Loop1 |
| | CsgA-24-TFF3_Loop2 |
| | CsgA-24-TFF3_Loop3 |
| | CsgA-24-TFF3_Loops1+2 |
| | CsgA-24-TFF3_Loops2+3 |
| | CsgA-48-TFF3_Loop1 |
| Short Synthetic Peptides | CsgA-48-T18 |
| | CsgA-48-CP15 |
| | CsgA-48-P8 |
| | CsgA-48-A1 |

Table 3: Engineered CsgA Constructs Library

To enable the exogenous control of the expression and assembly of the engineered curli fibers, the *csgA*-fusion gene must be placed under the control of an inducible promoter that will overexpress the fusion gene in the presence of the inducing chemical. For this study, the strong isopropyl $\beta$-D-1-thiogalactopyranoside (IPTG) inducible Trc promoter was used.

## 3.3 Materials & Methods

Note: Unless otherwise noted, the experiments for this chapter were conducted in collaboration with Dr. Anna Duraj-Thatte, Pichet Bom Praveschotinunt, and Fred Ward.

### 3.3.1 Strains & Plasmids

All cloning was conducted in Mach1 competent cells (Life Technologies, Carlsbad, CA, USA). All constructs were cloned into the pBbE1a plasmid (Lee et al., 2011), a ColE1 plasmid under control of the Trc promoter (Addgene, Cambridge, MA, USA). Figure 9 details the features of this pBpE1a plasmid. The *csgA* gene had already been isolated from *E. coli* K-12 genomic DNA and cloned into this plasmid, as previously described (Nguyen et al., 2014). Polymerase chain reaction and Gibson assembly were employed to open the plasmid and insert the functional peptide domains, as described below.

### 3.3.2 Synthesis of Peptide Insert Regions

The TFF1, TFF2, TFF3, and TFF3 loop sequence inserts were ordered as gBlocks and fully synthesized (Integrated DNA Technologies, Coralville, IA, USA). The specific sequences of each insert are included in Appendix 1. Different inserts were designed for use with different linkers so that Gibson assembly (Gibson et al., 2009) could be employed to insert them into plasmids already containing the *csgA* gene and linker sequence. The short synthetic peptide insert sequences were generated via overlap extension (Horton et al., 1989). Primers were designed to extend divergently from a region of homology to create the short inserts, that would have regions of homology with the desired plasmid on either end for incorporation with Gibson

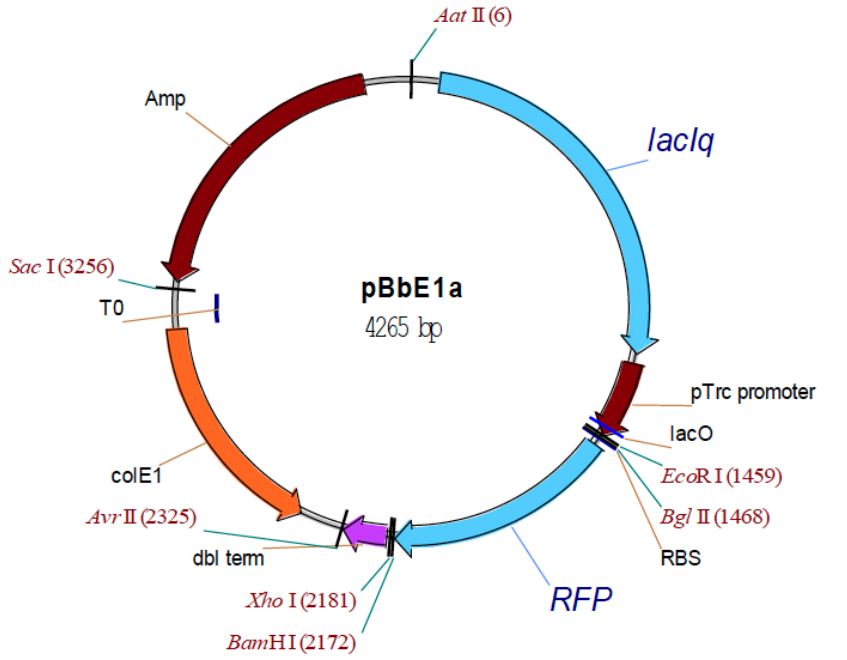


Figure 9: pBpE1a Plasmid Map. RFP is shown here in the open reading frame. Reproduced from Figure S3 of Lee et al., 2011

assembly. The sequences of these primers are included in Appendix 1. They were ordered and fully synthesized (Eurofins MWG Operon, Huntsville, AL, USA). Overlap extension was carried out using Phusion DNA Polymerase (New England BioLabs, Ipswitch, MA, USA), according to the manufacturer's protocol. Before using for Gibson assembly, these inserts were cleaned and concentrated using the Zymo Clean & Concentrator Kit (Zymo Research, Irvine, CA, USA), according to the manufacturer's protocol. Oligonucleotide concentrations were determined using a NanoDrop 2000c spectrophotometer (Thermo Fisher Scientific, Waltham, MA, USA).

### 3.3.3 Polymerase Chain Reaction

PCR was used to open the plasmid backbones for the insertion of the various functional inserts. Primers were designed to open the plasmid, retaining both the *csgA*

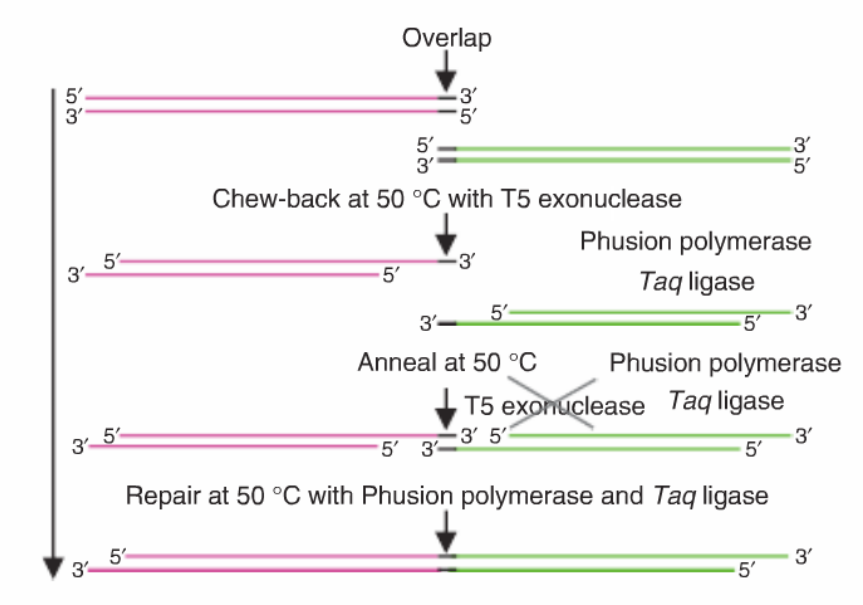


Figure 10: Overview of Gibson assembly. Reproduced from Figure 1 of Gibson et al., 2009

gene and the linker sequence. The sequences of these primers are included in Appendix 1. They were ordered and fully synthesized (Eurofins MWG Operon, Huntsville, AL, USA). PCR was conducted using Phusion DNA Polymerase (New England BioLabs, Ipswitch, MA, USA), according to the manufacturer's protocol. All PCR products were cleaned and concentrated using the Zymo DNA Clean & Concentrator Kit (Zymo Research, Irvine, CA, USA).

### 3.3.4 Gibson Assembly

Gibson assembly was carried out as previously described (Gibson et al., 2009), using the Gibson Assembly Master Mix (New England BioLabs, Ipswitch, MA, USA). Figure 10 describes the process of Gibson assembly.

### 3.3.5 Transformation

All engineered plasmids were transformed into competent Mach1 cells via electroporation using 0.1 cm GenePulser/MicroPulser electroporation cuvettes and the MicroPulser Electroporator (Bio-Rad Laboratories, Hercules, CA, USA). The "Ec1" electroporation setting was used. 50 $\mu$L aliquots of Mach1 cells were electroporated with 1 $\mu$L of DNA. Transformed cells were rescued with 1 mL of SOC outgrowth medium (New England BioLabs, Ipswitch, MA, USA), grown for 1 hour at 37°C and then plated on ampicillin selection plates, containing 25 g/L LB (Sigma-Aldrich, St. Louis, MO, USA) and 15 g/L agar (Becton, Dickinson & Co., Franklink Lakes, NJ, USA) supplemented with 100 mg/mL carbencillin (Teknova, Hollister, CA, USA) These plates were incubated overnight at 37°C.

### 3.3.6 DNA Sequencing

Transformed colonies grown overnight at 37°C were picked in triplicates and their plasmids were isolated using the QIAprep Spin Miniprep Kit (Qiagen, Hilden, Germany), following the manufacturer's protocols. The purified plasmids were mixed with the appropriate sequencing primers and sent for sequencing according to the provider's protocol (GENEWIZ, South Plainfield, NJ, USA). The sequences of these sequencing primers are shown in Appendix 1 and their binding sites on the pBpE1a plasmid are shown in Figure 11. After DNA sequencing, colonies containing the correct plasmid were inoculated in carbenicillin-supplemented LB media, grown overnight, and then prepared as glycerol stocks in 50% glycerol. These stocks were stored at -80° C.

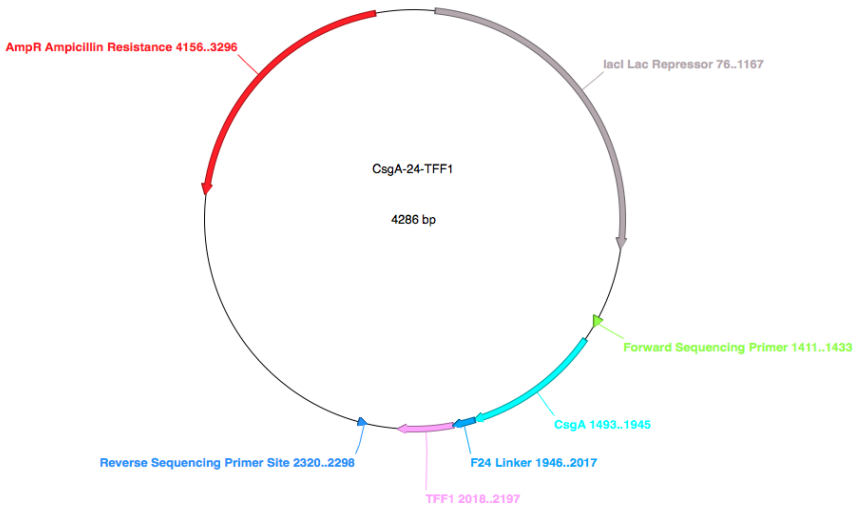


Figure 11: Overview of CsgA Construct Plasmids. The CsgA-24-TFF1 example shown here is representative of the entire library, with the *csgA* gene followed by a linker sequenced followed by the functional peptide, all within the open reading frame of the pBpE1a vector. The engineered section is also flanked by regions of homology with the two sequencing primers.

## 3.4 Results & Discussion

All of the desired constructs were able to be successfully engineered and cloned. As a first step, all of the insert sequences were successfully synthesized, as confirmed by the electrophoresis gel images shown in Figure 12. The visible DNA bands show that the insert sequences are the correct lengths (see Table 4 for the correct lengths of the inserts).

The plasmids containing the *csgA* gene and the different linker sequences were successfully opened using PCR, as shown by the electrophoresis gel image in Figure 13.

With these sequences and the ordered gBlocks, Gibson assembly was used to successfully assembly the inserts and open plasmids into closed circular vectors that were sequenced in triplicate to confirm successful assembly without mutations. The

| Insert | Sequence Length (bp) | Overlap Length on Either Side (bp) | Total Length (bp) |
|---|---|---|---|
| A1 | 21 | 30 | 81 |
| CP15 | 21 | 30 | 81 |
| P8 | 36 | 30 | 96 |
| T18 | 36 | 30 | 96 |
| TFF3 Loop 1 | 60 | 30 | 210 |
| TFF3 Loop 2 | 45 | 30 | 105 |
| TFF3 Loop 3 | 72 | 30 | 132 |

Table 4: Lengths of insert sequences.

| Linker in Vector | Sequence Length (bp) |
|---|---|
| F12 | 4,070 |
| F24 | 4,106 |
| F48 | 4,178 |

Table 5: Legnths of the opened pBpE1a plasmid with the *csgA* gene and various linkers.

sequencing results confirmed the successful construction of the entire library of CsgA fusion constructs.

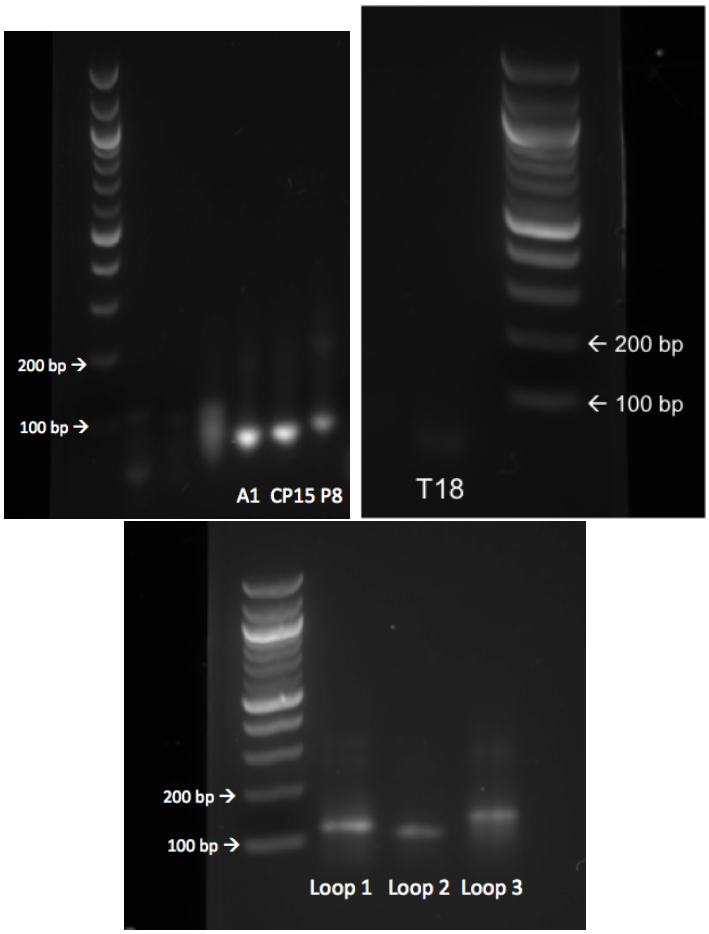


Figure 12: Confirmation of insert sequence synthesis by gel electrophoresis. A1, CP15, and P8 are shown in the top left, T18 is shown in the top right, and the TFF3 loops are shown at the bottom. 2% agarose TAE gel stained with SYBR Green.

# 4 Confirmation of Engineered Curli Fiber Expression

After genetically engineering plasmids to encode the production of functionalized biofilms, the curli fibers that are secreted and assembled must be analyzed to ensure the proper display of the desired peptides. To analyze these fibers, assays were conducted to (1) quantify curli expression and biofilm formation, (2) determine the size of the secreted CsgA-fusion monomers, and (3) immunohistochemically confirm the

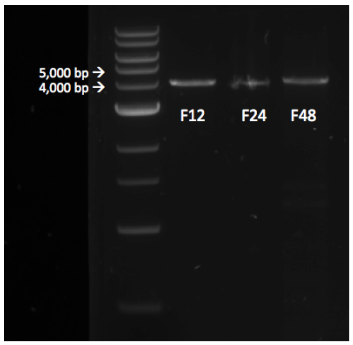


Figure 13: Confirmation of plasmid-opening PCR by gel electrophoresis. Plasmids containing the *csgA* gene and the three different linkers. 2% agarose TAE gel stained with SYBR Green.

identity of the displayed peptides.

## 4.1 Congo Red Staining for the Quantification of Curli Expression and Biofilm Formation

Assays for Congo red staining were conducted to determine the levels of curli expression and biofilm formation as compared with that of cells containing the wild type csgA gene in the same plasmid under the same promoter. The curli fibers expressed by the cells containing the engineered plasmids likely have the appended peptide since only the engineered fibers and not the wild type fibers are genetically encoded, so this assay serves as a good indication of successful secretion and assembly of the engineered fibers.

Congo red is a diazo amyloid-staining dye (Klunk et al., 1999) that has been used extensively as an colorimetric indicator of curli fiber expression and proper assembly in *E. coli* (Collinson et al., 1993; Nguyen et al., 2014). As has been described previously (Nguyen et al., 2014), bacterial cells harboring the engineered plasmid can either be grown in liquid culture and then treated with Congo red or grown on plates containing Congo red. The intensity of the red staining at 490 nm is proportional to the curli

fiber expression. For the liquid culture technique, liquid cultures induced overnight with IPTG were treated with Congo red and then centrifuged to pellet the cells. The reduction of Congo red dye in the supernatant as compared with a no bacteria negative control was indicative of curli expression. For the plate-based method, bacterial cells were simply grown to mid-log phase and then platted on plates containing Congo red as well as IPTG. The intensity of red staining was indicative of curli expression and biofilm formation. These results could be quantified using spectroscopy techniques, and all results could be normalized to that of the wild type for comparison. Both the liquid culture and plate-based methods were conducted for this study.

Scanning electron microscopy was also conducted to qualitatively confirm the presence of a biofilm surrounding the engineered bacterial cells. Morphological differences between the fibers displaying different peptides could be detected, contributing further to the confirmation that the desired peptides were displayed on the biofilm.

## 4.2 Identification of Displayed Peptides

It is possible that the functionalized addition to the curli fibers could be cleaved proteolytically during the secretion and assembly process. Therefore, further analysis was required to confirm that the desired peptide sequence is in fact displayed on the expressed curli fibers.

For molecular biology characterization techniques to be employed, it was first necessary to purify the secreted curli fibers from the rest of the cellular and extracellular milieu components. The robust nature of curli fibers was exploited for digestion in harsh detergents that would decompose the membranes, proteins, and nucleic acids of the expressing bacterial cells. In addition to purification, monomerization of the curli fibers was also required for many of the characterization techniques so that the

molecular weight of each CsgA-fusion construct could be determined.

Initial assays were conducted to confirm that the monomers of the displayed fibers had the correct molecular weight corresponding to the predicted molecular weight of the CsgA-fusion construct. These molecular weights were first determined by SDS-PAGE gel electrophoresis and subsequent staining with Coomassie Brilliant Blue. More accurate determinations of molecular weight were also made using matrix-assisted desorption/ionization (MALDI), a soft ionization mass spectrometry technique often used for the analysis of biomolecules. After molecular weight confirmation, western blotting was conducted with antibodies for TFF1, TFF2, and TFF3 to further confirm the identity of the displayed peptides. It is important to note, however, that the antibodies for TFF1, TFF2, and TFF3 bind to the C terminal tails of these peptides, which are not involved in the peptides' more complex tertiary structure (Thim, 1997), so it is possible that the displayed peptides could bind the antibody and their presence could be correctly confirmed by western blot, but they could be displayed in non-native and potentially non-active conformations. Therefore, western blotting is not entirely conclusive for proper conformational display of the peptides. Activity assays were conducted to gain insight into the biological activity of the displayed peptides.

Antibodies, unfortunately, were not available for the synthetic short peptides, but due to their short length, it is unlikely that they failed to be displayed if curli fibers were properly secreted and assembled into the biofilm. Therefore the proper display of these peptides was assumed after successful Congo red staining. The differences in the adhesion of bacteria expressing curli fibers engineered to display these peptides as compared with that of the wild type was seen as further evidence of proper peptide display.

## 4.3 Materials & Methods

Note: Unless otherwise specified, the experiments for this chapter were conducted in collaboration with Dr. Anna Duraj-Thatte and Pichet Bom Praveschotinunt.

### 4.3.1 Bacterial Strains

Curli fibers were expressed in two different *E. coli* strains, LSR10 and PHL628, both of which are *csgA* deletion mutants. LSR10 (MC4100, $\Delta csgA$) was a generous gift from the laboratory of Matthew R. Chapman (Department of Molecular, Cellular, and Developmental Biology, University of Michigan, Ann Arbor, MI, USA), and PHL628 (MGI655, *malA-Kan ompR234* $\Delta csgA$) cells were graciously donated by the laboratory of Anthony G. Hay (Department of Microbiology, College of Agriculture and Life Sciences, Cornell University, Ithaca, NY, USA). Neither strain produces cellulose, the other main component of the extracellular matrix secreted by most *E. coli* strains. This removes an element of complexity and allows the current study to focus on curli fibers as the main extracellular matrix component.

### 4.3.2 Transformation

The engineered plasmids were transformed into LSR10 and PHL628 cells as described in Section 3.3.5. Positive control cells were also transformed with the pBpE1a plasmid containing the wild type *csgA* gene without any linkers or appended peptide sequences, and negative control cells were transformed with a blank pBpE1a plasmid that did not contain the *csgA* gene. These positive control cells were referred to as wild type (WT), and the negative control cells were referred to as No CsgA (NC).

### 4.3.3 Bacterial Growth Media

LB media was composed of 10 g/L tryptone (Sigma-Aldrich), 5 g/L yeast extract (Sigma-Aldrich, St. Louis, MO), and 10 g/L NaCl (Sigma-Aldrich) in $H_2O$. YESCA media was composed of 10 g/L casaminoacids (Thermo Fischer Scientific) and 1 g/L yeast extract. These media were often supplemented with carbenicillin (Teknova) for bacterial selection. YESCA media was used during expression of curli due to it's low salt concentration, which has been shown to be beneficial for curli fiber production and biofilm formation (Nguyen et al., 2014). LB-agar plates were made from the LB media described above, supplemented with 15 g/L agar (Becton, Dickinson & Co.) and 200 ug/mL carbenicillin. YESCA-CR plates were made from the YESCA media described above, supplemented with 12 g/L agar, 200 $\mu$g/mL carbenicillin, 25 $\mu$g/mL Congo red (Sigma-Aldrich), 0.5 mM IPTG, and 3 $\mu$g/mL Coomassie Brilliant Blue R-250 (Thermo Fisher Scientific).

### 4.3.4 Curli Biofilm Formation

For curli expression, transformed cells were inoculated and grown in carbenicillin-supplemented (200 $\mu$g/mL) LB media to mid-log phase. The optical density at 600 nm ($OD_{600}$) of each sample was measured, and cultures were all normalized to $OD_{600}$ = 0.7 in carbencillin-supplemented (200 $\mu$g/mL) YESCA media. $OD_{600}$ measurements were taken with a NanoDrop 2000c spectrophotometer (Thermo Fisher Scientific). Cultures were induced with 0.3 mM IPTG and allowed to express overnight at 25°C with shaking. For plate based methods, inoculated cultures grown to mid-log phase were streaked or spotted onto YESCA-CR plates and incubated for 48 hours at 25°C.

### 4.3.5 Congo Red Staining Assays

After overnight induction, 1 mL from each culture was transferred to a 2 mL micro-centrifuge tube and centrifuged at 6,800g for 10 minutes at room temperature. The supernatant was removed by decanting and the cell pellet was resuspended in 1 mL PBS. 100 $\mu$L of 0.015 % was added to each sample, mixed gently, and incubated at room temperature for 10 minutes. For each assay, a negative control sample containing only PBS and 0.015 % Congo red without any cells was also prepared for reference. After incubation, all samples were pelleted at 14,000g for 10 minutes at room temperature. 150 $\mu$L from the supernatant of each sample, as well as of pure PBS and of the negative control sample without any cells, were added to a 96-well plate (Corning Inc., Corning, NY, USA). These samples were analyzed for absorbance at 490 nm, which is the maximum absorption wavelength for Congo red dye (Wu et al., 2012). Data were collected and analyzed using a BioTek Synergy H1 Multi-Mode Plate Reader and the accompanying Gen5 Data Analysis Software (BioTek Instruments, Inc., Winooski, VT, USA). Since this analysis indicates the level of Congo red remaining in the supernatant, the absorbance values for each sample were subtracted from that of the negative control sample without cells. This way, higher values were indicative of greater curli expression. For more useful comparison of relative levels of curli expression, all values were normalized to that of the samples from the positive control cells containing plasmids with the wild type *csgA* gene. This liquid cultured-based assay was referred to as the "Congo red spin down assay" for the purposes of this study.

For the plate-based Congo red spot test, inoculated cultures were spotted on to YESCA-CR plates containing IPTG and incubated for 48 hours at 25°C. These plates were then imaged, the intensity of the resulting images was analyzed using ImageJ

(National Institutes of Health, Bethesda, MD, USA; Schneider et al., 2012), and results were normalized to the wild type samples.

Note: Congo red assays were conducted in collaboration with Frederick Ward, a Harvard College undergraduate student working in the Joshi Laboratory.

### 4.3.6 Scanning Electron Microscopy

SEM images were taken as previously described (Nguyen et al., 2014). Briefly, induced cell samples were scrapped from YESCA-CR plates and resuspended in Millipore H2O, applied to Nucleopore filters with a 0.22 $\mu$m pore size (GE Healthcare Life Sciences, Pittsburgh, PA, USA) under vacuum, washed with $H_2O$ and fixed with 2% glutaraldehyde + 2% paraformaldehyde overnight at 4°C and then fixed in 1% osmium tetroxide. After washing with $H_2O$, the samples were dehydrated by an increasing ethanol gradient and then an increasing hexamethyldisilazane gradient. The samples were then gold sputtered and imaged on a Zeiss Supra55VP field-emission scanning electron microscope (Carl Zeiss, Inc., Thornwood, NY, USA). Pichet Bom Praveschotinunt generously provided all of the SEM images presented here.

### 4.3.7 Curli Fiber Purification

Multiple purification methods were implemented with varying degrees of success during this study. The first method implemented has been previously described (Nguyen et al., 2014; Romling et al., 2003). PHL628 transformants were grown on YESCA-CR plates for 72 hours and then scrapped and resuspended in 2.5 mL tris-buffered saline (TBS). Sonication with a Qsonica Q700 Sonicator (Qsonica, LLC, Newtown, CT, USA) was used to shear the curli fibers from the bacterial cells. The program used applied 15% power in 30s pulse/2 minutes rest cycles repeated for a total process time of 3 minutes. The sonicated cells were pelleted by centrifugation at 3,600g for 20

minutes and then the supernatant was collected and treated with 1% sodium dodecyl sulfate (SDS) and 250 mM NaOH for 1 hour at room temperature with shaking. The remaining insoluble fraction was pelleted by ultracentrifugation at 120,000g for 45 minutes in a Beckman Coulter Optima XPN Preparatory Ultracentrifuge (Beckman Coulter, Inc., Indianapolis, IN, USA). The resulting pellet was resuspended in 5 mL Millipore $H_2O$ and then pelleted again at 120,000g for 45 minutes. This wash step was repeated once more. The final pellet was resuspended in 100 $\mu$L Millipore $H_2O$ and lyophilized overnight in a Sentry 2.0 lyophilizer (SP Scientific, Warminster, PA, USA).

For the second purification method transformed PHL628 cells grown for 72 hours on YESCA-CR plates were scrapped off and resuspended in 2 mL PBS. These samples were pelleted by centrifugation at 14,000g for 20 minutes. The resulting pellet had a distinct layer on the top that is hypothesized to be curli fibers stained with Congo red. This layer was carefully scrapped off and resuspended in 200 $\mu$L of BugBuster solution (EMD Millipore, Billerica, MA, USA), supplemented with 1 $\mu$L/mL Benzonase nuclease (Sigma-Aldrich, St. Louis, MO, USA) and 0.25 mg/mL lysozyme (40,000 units/mg; Sigma-Aldrich). The sample were incubated at room temperature for 20 minutes with shaking and then pelleted by centrifugation at 14,000g for 30 minutes at 4°C. The supernatant was decanted and then the pellet was resupended again in 200 $\mu$L of supplemented BugBuster solution and incubated again at room temperature with shaking for 20 minutes. After pelleting again at 14,000g for 30 minutes, the samples were resuspended in 500 $\mu$L PBS to wash the remaining lysozyme off the purified fibers. The samples were pelleted one last time at 14,000g for 30 minutes, resuspended in 100 $\mu$L H2O and then lyophilized overnight in a Sentry 2.0 lyophilizer (SP Scientific).

### 4.3.8 CsgA-Fusion Monomerization

After purification, curli fiber samples were digested into monomers for further analysis, as previously descrved (Nguyen et al., 2014). Lyophilized purified curli fibers were resuspended in 100 $\mu$L hexaflouro-2-propanol (HFIP; Oakwood Chemical, Denver, CO), which has been used in previous studies to dissolve amyloid fibers (Zhou et al, 2013). The samples were incubated at room temperature with shaking for 1 hour and then the solvent was evaporated using a Savant SpeedVac SPD131DDA (Thermo Fisher Scientific, Waltham, MA, USA) set at 55°C for 1 hour.

### 4.3.9 SDS-PAGE Analysis

The approximate molecular weight of CsgA-fusion monomers could be determined using SDS PAGE (polyacrylamide gel electrophoresis) and subsequent staining with Coomassie Brilliant Blue dye. Lyophilized purified culrli fiber samples were weighed and resupended in Millipore $H_2O$ to a concentration of 10 mg/mL and then prepared for SDS PAGE. Samples were mixed with an equivalent volume of 2X Laemmli Sample Buffer (Bio-Rad Laboratories, Hercules, CA, USA) and then boiled at 95°C for 10 minutes. 10 $\mu$L of prepared sample were added per well in Mini-PROTEAN TGX Any kD precast gels (Bio-Rad Laboratories). 10 $\mu$L of Precision Plus Protein Standards ladder solution (Bio-Rad Laboratories) was added to one well of each gel. The gels were run in with tris/glycine/SDS electrophoresis buffer (Bio-Rad Laboratories) at 200V for 50 minutes and then dyed with Coomassie Brilliant Blue dye (2.5 mg/L CBB in 50% MeOH, 40% H2O, 10% acetic acid solution). After staining for 1 hour at room temperature with gentle shaking, gels were incubated with destaining solution (50% MeOH, 40% H2O, 10% acetic acid) for another hour with gentle shaking and then imaged using a FlourChem M Imaging System (Protein Simple, San Jose, CA, USA).

### 4.3.10 MALDI Analysis of Dissolved Extracellular Fractions

MALDI was conducted as previously described (Nguyen et al., 2014). Briefly, monomerized CsgA-fusion samples were dissolved in a minimal volume of 1:1 acetonitrile-$H_2O$ with 0.1% triflouroacetic acid (TFA; Sigma-Aldrich, St. Louis, MO, USA) and then applied to the sample plate using the sandwich method. Sinapinic acid (Thermo Fisher Scientific, Waltham, MA, USA) was used as the MALDI matrix, as previously described (Kussmann et al., 1997). The samples were analyzed using a Bruker ultrafleXtreme MALDI-TOF/TOF mass spectrometer (Bruker Corporation, Billerica, MA, USA). Pei Kun Richie Tay, a bioengineering Ph.D. candidate in the Joshi Laboratory, generously conducted all MALDI data collection.

### 4.3.11 Western Blotting for Trefoil Factor Family Peptides

Antibodies were purchased for TFF1 (Abcam, Cambridge, UK), TFF2 (R&D Systems, Minneapolis, MN, USA), and TFF3 (Alpha Diagnostics International, San Antonio, TX). Purified and monomerized CsgA-fusion protein samples were resuspended to 10 mg/mL in Millipore $H_2O$ and prepared for gel electrophoresis. For every 10 $\mu$L of prepared sample, 6.5 $\mu$L of purified and suspended CsgA-fusion protein was mixed with 2.5 $\mu$L 4X NuPAGE LDS Sample Buffer and 1 $\mu$L 10X NuPAGE Reducing Agent (both from Life Technologies, Carlsbad, CA, USA) and then boiled at 95°C for 10 minutes. Samples were added to NuPAGE Bis-Tris Mini Gels (Life Technologies) with 10 $\mu$L per well. A ladder (Life Technologies) was also added to one well in each gel. The gels were run in nuPAGE MES SDS Running Buffer (Life Technologies) at 200V for 35 minutes. After run completion, the proteins from each gel were transferred to polyvinylidene fouride (PVDF) membranes using an iBlot Gel Transfer Device and iBlot Gel Transfer Stacks (Life Technologies). After protein transfer, the membranes

were incubated in blocking solution (50 g/L milk protein in tris-buffered saline with Tween20 (TBST)) for 1 hour with shaking before the membranes were treated with the appropriate antibody, diluted 1:1000 in TBST. The membranes were incubated with antibodies overnight with shaking at 4°C and then washed with TBST. The secondary antibody (details here; a horseradish peroxidase (HPR) conjugated antibody; different for TFF1, right?) was added to each membrane with 1 $\mu$L in 50 mL TBST and incubated for 1 hour at room temperature with shaking. The Clarity Western Blotting Substrate Kit (Bio-Rad Laboratories, Hercules, CA, USA) was used to activate the luminescence of the HRP conjugated to the secondary antibodies. The membranes were imaged using a FlourChem M Imaging System (Protein Simple, San Jose, CA, USA).

### 4.3.12 Statistical Analysis

All statistical analysis was conducted in MATLAB (Mathworks,Natick, MA, USA). P values were generated using a two-sample Student's t test with the MATLAB ttest2 function. All plots were also generated with MATLAB.

## 4.4 Results & Discussion

### 4.4.1 Engineered Curli Fiber Expression

The Congo red spin down assays confirmed the successful secretion of curli fibers in transformants for the majority of the engineered constructs. As can be seen in Figure 14, transformants of all of the constructs designed to display the short synthetic peptides (A1, P8, T18, and CP15) were able to express, secrete, and assemble curli fibers at a level comparable to that of transformants expressing unmodified wild type curli fibers, with curli expression measured by the reduction in absorbance at

490 nm in the supernatant of centrifuged sample containing the transformed E. coli. There was no statistically significant difference between the expression of these short peptide-modified curli fibers and the wild type curli fibers, but the expression of all of these curi fibers, modified and unmodified, was statistically significantly greater than that of the No CsgA transformants containing the empty pBpE1a vector (see Table 6 for p-values).

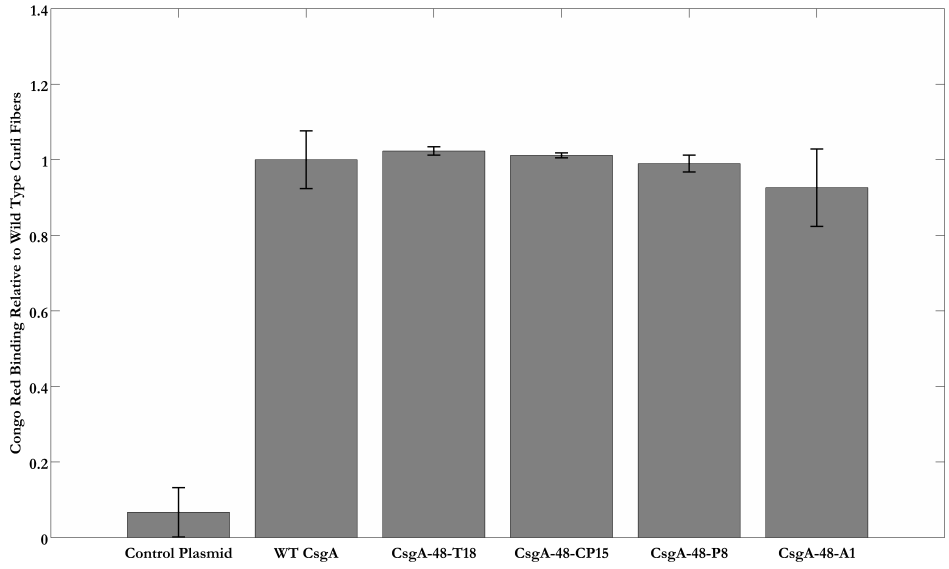


Figure 14: Congo red staining as a measure of the expression of curli fibers displaying the short synthetic peptides in LSR10 *E. coli*. All data are relative to the expression of unmodified wild type curli fibers. Error bars represent standard deviation. Performed in triplicate ($n = 3$)

As can been seen in Figures 15 and 16, the curli fiber expression for the transformants expressing CsgA appended to the TTF peptides has greater variation than that of the short synthetic peptides, but the majority of the constructs have statistically significantly greater curli expression than the control vector, so they are all expressing curli, but these expression levels are not as similar to wild type expression as those of the short peptides (see Table 7 for p-values).

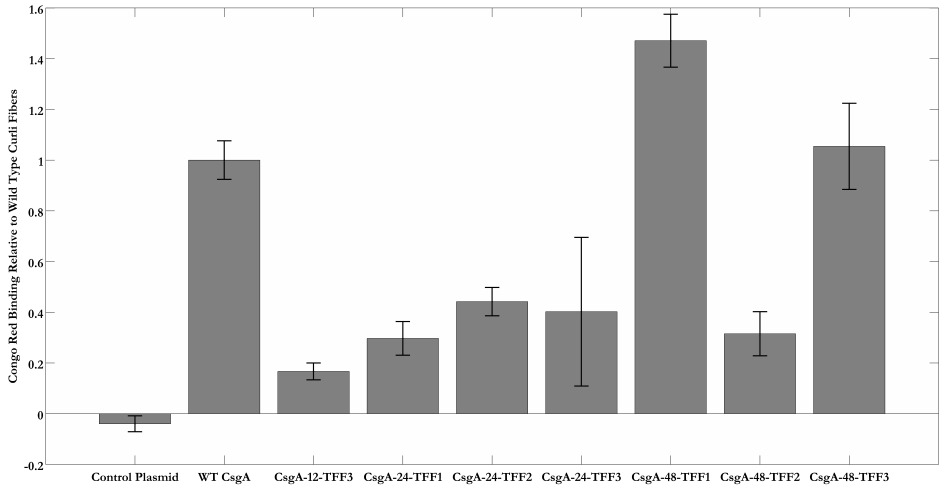


Figure 15: Congo red staining as a measure of the expression of curli fibers displaying the trefoil family factor peptides in LSR10 *E. coli*. All data are relative to the expression of unmodified wild type curli fibers. Error bars represent standard deviation. Performed in triplicate ($n = 3$)

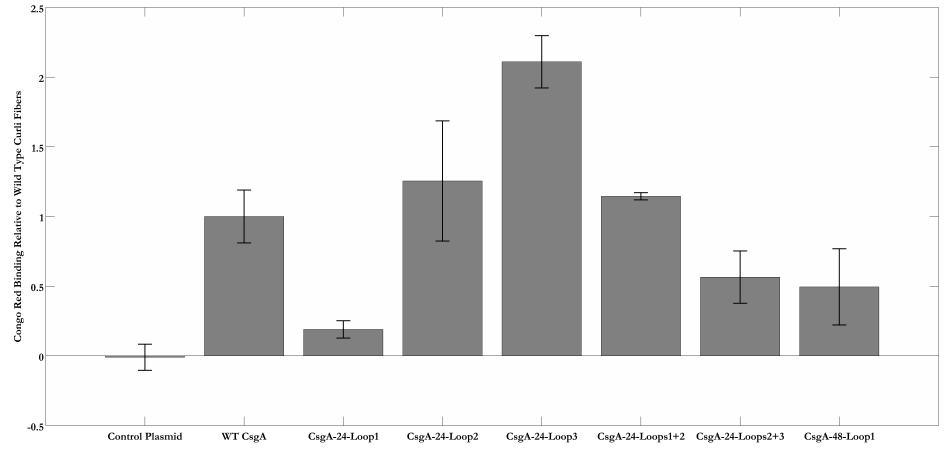


Figure 16: Congo red staining as a measure of the expression of curli fibers displaying the TFF3 loops in LSR10 *E. coli*. All data are relative to the expression of unmodified wild type curli fibers. Error bars represent standard deviation. Performed in triplicate ($n = 3$)

The lower values of TFF-modiefied curli fibers expression was likely due to difficulty secreting the large CsgA-TFF monomers and subsequent toxicity to the cell

upon build up of these monomers within the periplasm. Growth curve studies (data not shown) confirmed this hypothesis that the TFF-modified curli fibers were in fact somewhat toxic to the expressing *E. coli*, with the growth of these transformants slowing after induction.

| Construct | Comparison to Wild Type | Comparison to Control Plasmid |
|---|---|---|
| CsgA-48-T18 | p= 0.630 | p< 0.001 |
| CsgA-48-CP15 | p= 0.806 | p< 0.001 |
| CsgA-48-P8 | p= 0.836 | p< 0.001 |
| CsgA-48-A1 | p= 0.373 | p< 0.001 |

Table 6: Statistical Significance of Short Peptide-Modified Curli Fiber Expression in LSR10 *E. coli* (Induction with 0.3mM IPTG)

All of the curli fiber expression discussed above was obtained from LSR10 strain E. coli transformants, but as experiments continued, the LSR10 strain became somewhat pragmatically problematic. Cultures began to drop engineered plasmid, even with increased dosages of carbenicillin, so studies were transferred to a very similar E. coli strain, PHL628, which also has the *csgA* deletion and does not produce additional extracellular matrix material. This strain was used for the production of the curli fibers that were purified and used for subsequent assays. This strain was also used for the SEM images shown in the next section.

It was also observed that the TFF construct plasmids had significant leaking, with TFF-modified curli fiber expression observed prior to IPTG induction, which was likely due to the toxicity issues discussed above. Therefore, for the Congo red assay conducted with the PHL628 strain, the liquid cultures were supplemented with 2% glucose, a repressor for the lac operon promoter in the pBpE1a plasmid , during the inoculation growth phase, limiting curli expression before induction. This dra-

| Construct | Comparison to Wild Type | Comparison to Control Plasmid |
|---|---|---|
| CsgA-24-TFF1 | p< 0.001 | p= 0.0014 |
| CsgA-24-TFF2 | p< 0.001 | p< 0.001 |
| CsgA-24-TFF3 | p= 0.027 | p= 0.060 |
| CsgA-12-TFF3 | p< 0.001 | p= 0.0014 |
| CsgA-48-TFF1 | p= 0.003 | p< 0.001 |
| CsgA-48-TFF2 | p< 0.001 | p= 0.0027 |
| CsgA-48-TFF3 | p= 0.639 | p< 0.001 |
| CsgA-24-Loop1 | p= 0.002 | p= 0.037 |
| CsgA-24-Loop2 | p= 0.402 | p= 0.008 |
| CsgA-24-Loop3 | p= 0.002 | p< 0.001 |
| CsgA-24-Loops1+2 | p= 0.260 | p< 0.001 |
| CsgA-24-Loopes2+3 | p= 0.048 | p= 0.009 |
| CsgA-48-Loop1 | p= 0.058 | p= 0.039 |

Table 7: Statistical Significance of TFF-Modified Curli Fiber Expression in LSR10 *E. coli* (Induction with 0.3mM IPTG)

matically improved TFF-modified curli expression after induction. As can be seen in Figure 17, curli fiber expression in PHL628 with 2% was more uniform across the constructs in comparison to wild type expression. The expression of all of these curi fibers, modified and unmodified, was statistically significantly greater than that of the No CsgA transformants containing the empty pBpE1a vector. Although there were statistically significant differences between the modified curli fibers and the wild type fibers, the plot in Figure 17 reveals that all of these modified curli fibers have expression levels slightly less than that of the wild type fibers. This significance, therefore, was likely due to the small error associated with these data and their

narrow distributions. Results are only presented for the four constructs (CsgA-48-TFF1, CsgA-24-TFF2, CsgA-24-TFF3, and CsgA-48-T18) that were focused on for the downstream curli analysis. Overall, this shows that these constructs have strong modified curli production, very similar to that of wild type curli, strongly indicating that these fibers are displaying the desired peptides and are suitable for further analysis.

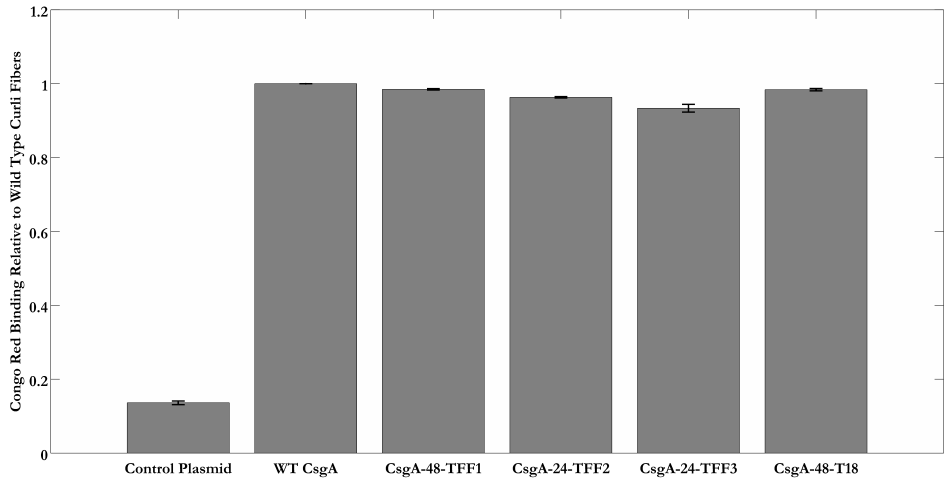


Figure 17: Congo red staining as a measure of the expression modified curli fibers in PHL628 *E. coli*. Bacteria were induced with 2% glucose and 0.3mM IPTG. All data are relative to the expression of unmodified wild type curli fibers. Error bars represent standard deviation. Performed in triplicate ($n = 3$)

### 4.4.2 Scanning Electron Microscopy Analysis

SEM images further qualitatively confirmed the expression of the modified curli fibers. As can be seen in Figures 18 and 19, the transformants expressing wild type and engineered curli are surrounded by small fibers, embedding the cells in a mesh-like curli matrix, while the No CsgA transformants without the csgA gene are not surrounded by any visible extracellular matrix materials. Additionally, morphological differences

between the wild type curli fibers and the TFF-modified curli fibers can be seen, with the TFF-modified fibers forming denser matrices, consistent with their larger CsgA-fusion monomer sizes, further confirming the display of these peptides on the engineered fibers.

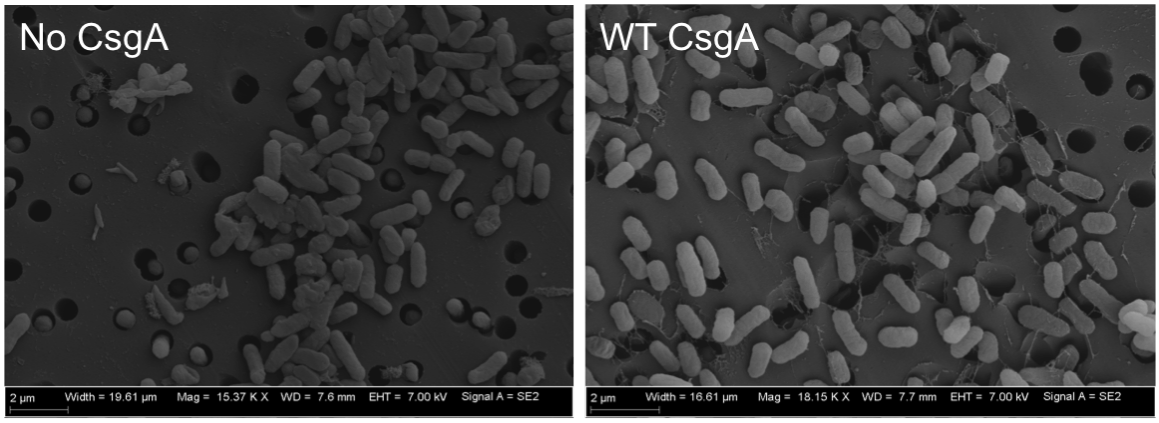


Figure 18: SEM Images of *E. coli* cells with and without unmodified curli fibers. Note the small fibers surrounding the cells expressing wild type CsgA. Scale bars are shown in the bottom left of each individual image.

Due to experimental constraints, SEM images were only obtained for WT CsgA, No CsgA, CsgA-48-TFF1, CsgA-24-TFF2, CsgA-24-TFF3, and CsgA-48-T18, the library members that were investigated in subsequent adhesion and biological activity assays. Additional SEM images of transformants expressing these constructs can be found in Appendix XX. (N.B. All SEM images were taken by Pichet Bom Praveschotinunt and used with permission).

### 4.4.3 Molecular Weight Analysis of CsgA-Fusion Monomers

Before analysis of the molecular weights of the CsgA-fusion monomers could be conducted, the engineered curli fibers needed to be purified and dissolved into monomers. A new purification protocol had to be developed for this study, and this protocol produced initially successful results (Figure 20), but these results were not duplicated by

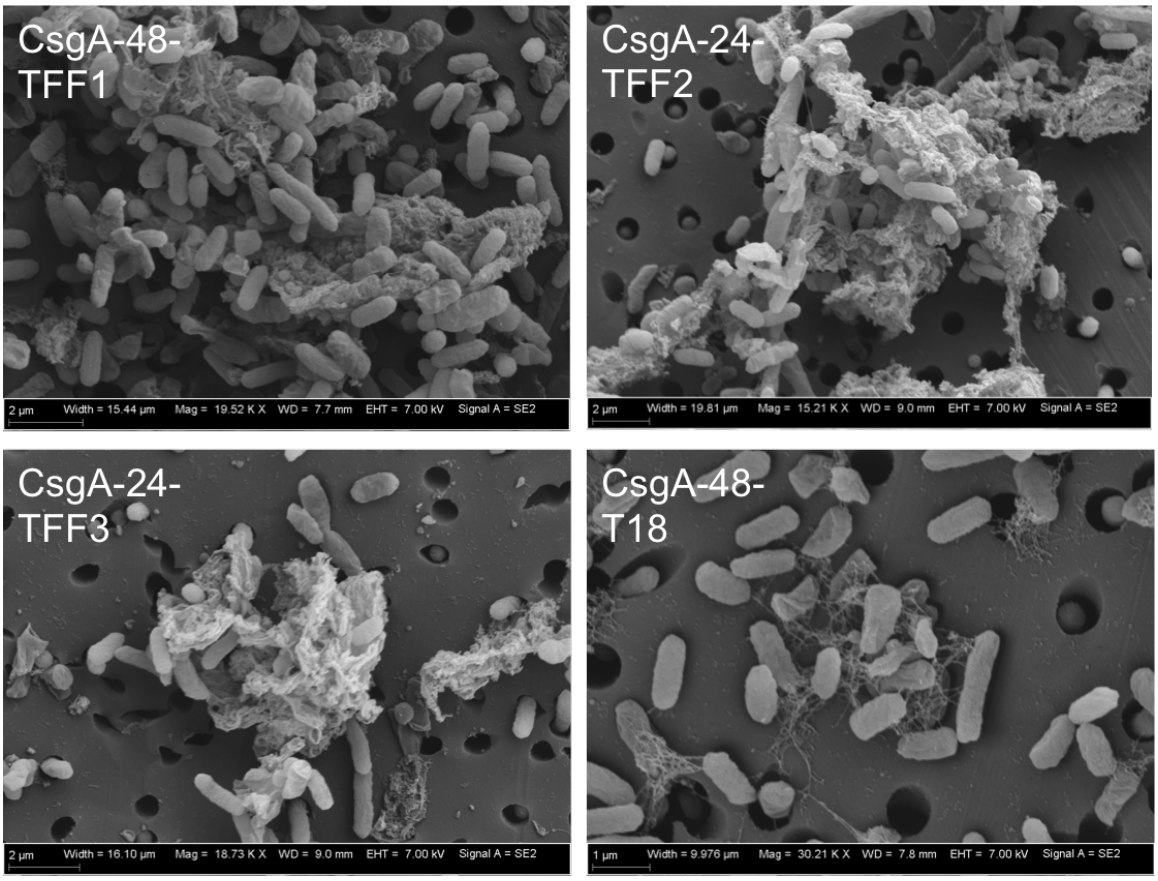


Figure 19: SEM Images of *E. coli* cells expressing four of the CsgA constructs: CsgA-48-TFF1, CsgA-24-TFF2, CsgA-24-TFF2, and CsgA-48-T18. Note the differences between the morphologies of the TFF-modified curli fibers and the wild type fibers in Figure 18. The T-18-modified fibers, however, look similar to the wild type fibers due to the small size of the displayed peptide. Scale bars are shown in the bottom left of each individual image.

subsequent purifications. These differences were actually likely due to the monomerization process, rather than the purification process. The samples for this first SDS-PAGE analysis were incubated in HFIP overnight for monomerization, which likely dissolved more of the remaining cellular and extracellular components not dissolved by the purification process. Since many of the downstream applications of the purified curli fibers required full, polymerized curli fibers, additional incubation in HFIP was not seen as a viable purification protocol. Even though ultra-pure curli fiber samples

were not obtained, subsequent assays were still conducted with these relatively pure samples, since the purification definitely removed all living components of the cultures and the majority of the cellular debris.

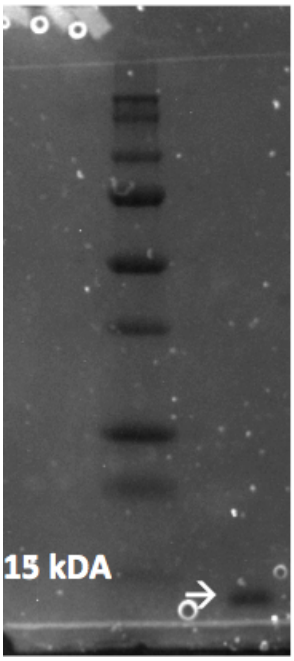


Figure 20: SDS-PAGE analysis of purified wild type CsgA. The 15 kDa ladder level is labeled and the CsgA band at approximately 13 kDa is indicated with an arrow. The purification was deemed successful due to the lack of other signiciant bands.

Once CsgA-fusion monomers were obtained, SDS-PAGE was conducted to confirm the molecular weights of these constructs. Since the short synthetic fibers are so small, an appreciable difference in molecular weight between these fibers and the wild type CsgA monomers would be difficult to observe via SDS-PAGE, so only the TFF-modified CsgA monomers underwent SDS-PAGE. Specifically, the CsgA-48-TFF1, CsgA-24-TFF2, and CsgA-24-TFF3 constructs were analyzed. As can be seen in Figure 21, SDS-PAGE analysis revealed that all of the samples of semi-purified CsgA-TFF monomers contained proteins of the predicted molecular weights (see Table 8 for the predicted molecular weights of the CsgA-TFF monomers).

| CsgA-Fusion Monomer | Predicted Molecular Weight |
|---|---|
| WT CsgA | 13 kDa |
| CsgA-48-TFF1 | 22.7 kDa |
| CsgA-24-TFF2 | 26.5 kDa |
| CsgA-24-TFF3 | 21.1 kDa |

Table 8: Predicted molecular weights for wild type CsgA and three of the CsgA-TFF construct monomers.Molecular weights were predicted using the online ProtParam tool on ExPASy, the Swiss Bioinformatics Resource Portal, at web.expasy.org/protparam/

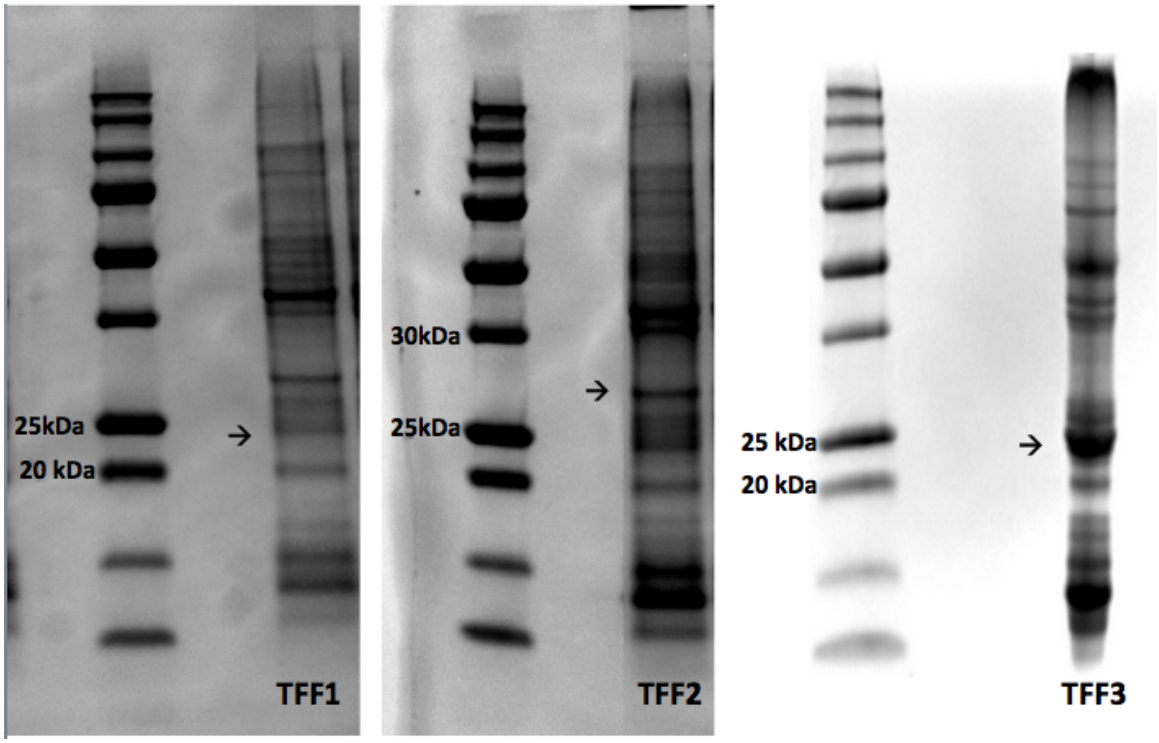


Figure 21: SDS-PAGE analysis of the molecular weights of CsgA-48-TFF1 (left), CsgA-24-TFF2 (middle), and CsgA-24-TFF3 (right). Ladders are shown to the left of each sample lane. Bands at the appropriate predicted molecular weights are indicated with arrows.

Following SDS-PAGE analysis, matrix-assisted desorption/ionization (MALDI) was employed to further confirm the molecular weights at a higher resolution. However, due to the purification issues described above, clean MALDI reads were difficult

to obtain, but Figure 22 shows the results from purified wild type CsgA. The peak at approximately 13 kDa confirms the presence of CsgA. (N.B. All MALDI data was collected by Pei Kun Richie Tay and used with permission).

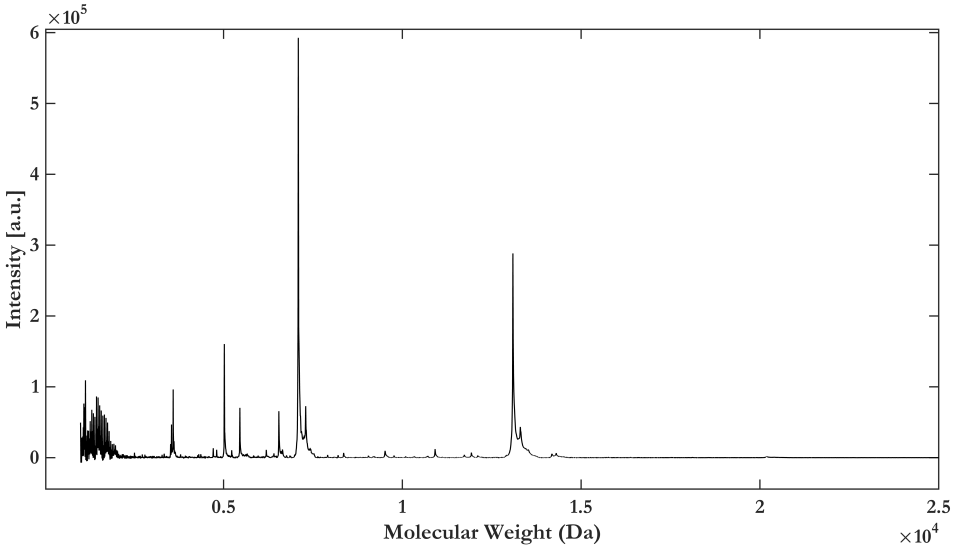


Figure 22: MALDI analysis of wild type CsgA. The peak at approximately 13 kDa corresponds with CsgA, but the presence of other significant peaks demonstrates that the sample is not entirely purified.

### 4.4.4 Western Blotting for Display of Trefoil Factor Family Peptides

Upon confirmation of correct molecular weight by SDS-PAGE, the semi-purified CsgA-TFF monomers were immunoblotted with human TFF1, TFF2, and TFF3 antibodies to immunohistochemically confirm the identity of the peptides displayed on the curli fibers. As can be seen in Figure 23, curli-displayed TFF2 and TFF3 peptides were successfully identified by Western blotting. The additional bands are the result of non-specific antibody binding due to the lack of optimization of the required antibody concentration. Future ongoing work will optimize this concentration to reduce such non-specific bands. The bands seen at multiples of the predicted monomer molecular weights are likely due to incomplete monomerization of the curli fibers. The

band seen at the top of the TFF3 image is likely due to the aforementioned clumping of monomers that would not resuspend, and as a result could not move through the gel. Due to time constraints, western blotting with the anti-TFF1 antibody was not conducted, but will easily be conducted in future work.

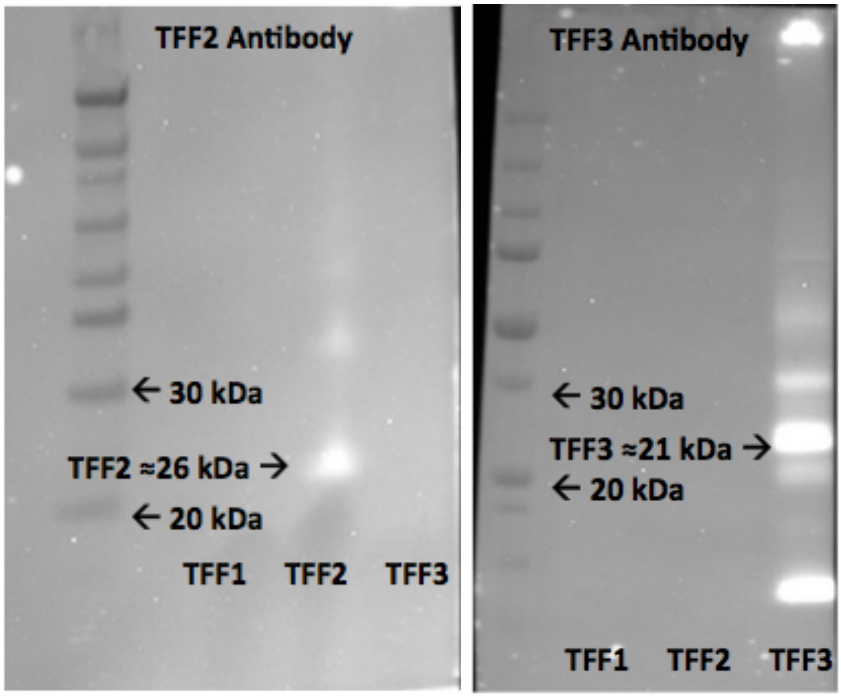


Figure 23: Western blotting to detect TFF2 and TFF3 displayed on engineered curli fibers. The membrane on the left was treated with human TFF2 antibody and the membrane on the right was treated with human TFF3 antibody.Each membrane contains CsgA-48-TFF1, CsgA-24-TFF2, and CsgA-24-TFF3 in three lanes labeled at the bottom. Ladders are shown to the left of the sample lanes. Bands at the appropriate predicted molecular weights are indicated.

As previously mentioned, it is important to note that the antibodies for TFF1, TFF2, and TFF3 bind to the C terminal tails of these peptides, which are not involved in the peptides' more complex tertiary structure (Thim, 1997), so it is possible that they could be displayed on the curli fibers and identified by western blotting, but not necessarily be in an active conformation.

In conclusion, the work presented in this chapter confirms that *E coli* trans-

formants of at least one CsgA-fusion construct for each desired peptide were able to secrete curli fibers. SDS-PAGE analysis further confirmed the correct molecular weights of CsgA-TFF1, CsgA-TFF2, and CsgA-TFF3 construct monomers, and western blotting identified the presence of TFF2 and TFF3 on curli fiber monomers. This was considered sufficient evidence of proper peptide-modified curli fiber expression to progress to downstream assays concerning adhesion and peptide biological activity.

## 4.5 Future Work

Future work will first need to improve the purification procedure so that MALDI and cleaner SDS-PAGE analysis can be conducted. The addition of a gel purification step would likely prove beneficial. Resolving the resuspension issues associated with the monomerization process will also likely improve this analysis. New monomerization protocols using formic acid or $NH_4OH$ should be explored, as these protocols have been reportd in the literature for dissolving amyloid fibers. Western blotting with the TFF1 antibody should also be conducted to further confirm the display of TFF1 on curli fibers, and SDS-PAGE and MALDI analysis with more of the constructs should be conducted to provide more supporting eveidence that the short peptides and TFF3 loops are indeed properly displayed on curli fibers.

# 5 Effect of Functionalized Curli Fibers on Bacterial Adhesion to Epithelial Cells

When commensal microflora colonize the human gastrointestinal tract, they often adhere to the epithelial cells lining the intestinal lumen to improve their fitness and help them out-compete other organisms for colonization success. It is hypothesized, therefore, that controlling this epithelium adhesion can be used to modulate the localization of and spatiotemporal dynamics of bacteria. A first step to achieving such control is engineering bacteria have increased adhesion to gastrointestinal epithelial cells through the biofilm display of peptides with inherent affinity for the intestinal epithelium. The trefoil factor family peptides and short synthetic peptides investigated in this study were selected in part due to such inherent affinity, so adhesion assays were conducted to determine whether the display of these peptides on curli fibers would in fact improve the intestinal epithelium ahehesion of transformant *E. coli* expressing them. These assays were based on previously described methods for the study of bacterial adhesion to epithelial cells (Puttamreddy et al., 2011; Letourneau et al., 2011) and were conducted using the CaCo-2 cell line, a human epithelial colorectal adenocarcinoma-derived cell line frequently used for in vitro studies of the human gastrointestinal tract.

## 5.1 Materials & Methdods

### 5.1.1 Mammalian Cell Lines and Culture Conditions

CaCo-2 cells were grown in culture according to previously described best practices (Natoli et al., 2012). Dulbecco's Modified Eagle Medium (DMEM) supplemented with 4.5 g/L D-glucose and L-glutamine but without sodium pyruvate (Gibco, Life

Technologies, Carlsbad, CA, USA) was the standard base culture medium used, and future instances of DMEM in the text refer to this DMEM formulation. Cells were grown in DMEM supplemented with 15% fetal bovine serum (Gibco, Life Technologies, Carlsbad, CA, USA) and 1% pen/strep solution (5,000 units/mL of penicillin and 5000 $\mu$g/mL of streptomycin; Gibco, Life Technologies, Carlsbad, CA, USA) in T75 tissue culture flasks (Corning Inc., Corning, NY, USA). Cells were incubated at 37°C with 5% CO2 . Cells were treated with trypsin-EDTA (Gibco, Life Technologies, Carlsbad, CA, USA) and passaged with a 1:20 dilution approximately every 72 hours.

### 5.1.2 Adhesion Assays

After passaging, 1 x $10^5$ CaCo-2 cells were added to each well of a 24-well tissue culture plate (Corning, Inc., Corning, NY, USA) in 500 $\mu$L DMEM supplemented with 15% FBS and 1% pen/strep solution and incubated at 37°C with 5% CO2 for 48 hours until 90% confluent. At the same time, LSR10 *E. coli* cells transformed with the appropriate CsgA-fusion constructs were induced in carbenicillin-supplemented (200 $\mu$g/mL) YESCA media with 0.3 mM IPTG and allowed to express for 48 hours at 25°C. Bacterial cultures were normalized to OD_600 = 0.1 in fresh DMEM media, which corresponds to approximately 1 x $10^7$ colony forming units (C.F.U) per mL, and then 90% confluent CaCo-2 cells were infected with 1 mL of this bacterial solution per well. The cells and bacteria were co-cultured at 37°C and 5% CO_2 for either 6 or 24 hours, then the media was removed, and the cells were washed twice with 200 $\mu$L PBS per well, before being treated with trypsin-EDTA to remove the mammalian cells and adherent bacterial cells from the plate. These samples were serially diluted in PBS and then plated on carbenicillin-supplemented (200 $\mu$g/mL) LB agar plates and incubated overnight at 37°C. Bacterial colonies were counted and weighted ap-

propriately, depending on the dilution, to determine the C.F.U. of adhered bacteria for each construct.

### 5.1.3 Data Analysis

All statistical analysis was conducted in MATLAB (Mathworks,Natick, MA, USA). P values were generated using a two-sample Student's t test with the MATLAB ttest2 function. All plots were also generated with MATLAB. Relative adhesion was determined by dividing the C.F.U reported for each construct by the C.F.U for wild type CsgA.

## 5.2 Results & Discussion

Adhesion assays were conducted with LSR10 *E. coli* transformants expressing wild type CsgA, CsgA-48-TFF1, CsgA-48-TFF2, CsgA-48-TFF3, CsgA-48-T18, CsgA-48-A1, CsgA-48-CP15, and CsgA-48-P8. The two assays were conducted with co-culture incubation times of 6 hours and and 24 hours, respectively, as shown in Figures 24 and 25. All of the constructs are not listed for both assays due to incidental issues with inoculation and induction prior to the start of each assay that prevented the inclusion of some constructs.

| Construct | Comparison to Wild Type Curli Adhesion |
|---|---|
| CsgA-48-TFF3 | p= 0.065 |
| CsgA-48-T18 | p= 0.002 |
| CsgA-48-A1 | p= 0.517 |
| CsgA-48-CP15 | p= 0.270 |
| CsgA-48-P8 | p= 0.477 |

Table 9: Statistical significance of six hour adhesion studies with LSR10 *E. coli* and CaCo-2 mammalian cells.

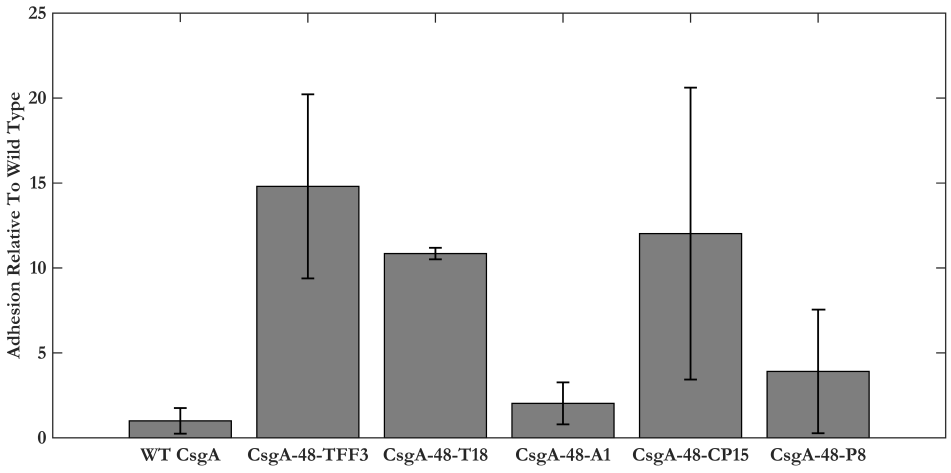


Figure 24: Six hour adhesion assay demonstrates improved adhesion with some modified curli fiber variants over wild type curli fibers. All samples were in triplicate, $n = 3$, and error bars represent $\pm$ standard error of the mean.

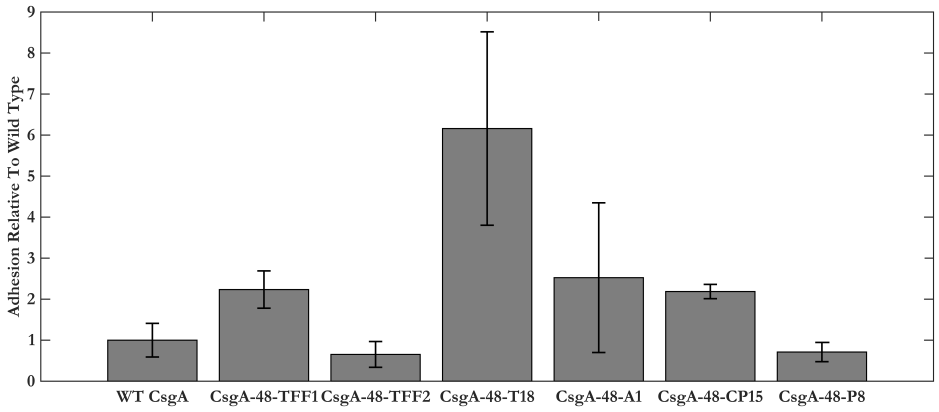


Figure 25: Twenty four hour adhesion assay demonstrates improved adhesion with some modified curli fiber variants over wild type curli fibers. All samples were in triplicate, $n = 3$, and error bars represent $\pm$ standard error of the mean.

As can be seen in these figures and the corresponding tables of p values, bacterial cells expressing curli fibers modified with T18 had statistically significant improved adhesion as compared to bacteria expressing wild type curli. TFF3 and CP15 modified curli fibers also showed promise in the six hour and twenty four hour studies,

respectively, but future reduction in sample variability will be required to make these results statistically significant.

| Construct | Comparison to Wild Type Curli Adhesion |
|---|---|
| CsgA-48-TFF1 | p= 0.114 |
| CsgA-48-TFF2 | p= 0.539 |
| CsgA-48-T18 | p= 0.097 |
| CsgA-48-A1 | p= 0.461 |
| CsgA-48-CP15 | p= 0.056 |
| CsgA-48-P8 | p= 0.574 |

Table 10: Statistical significance of 24 hour adhesion studies with LSR10 *E. coli* and CaCo-2 mammalian cells.

## 5.3 Future Work

More adhesion assays will need to be conducted to confirm the findings presented here. It should be noted that the error bars are quite large for many of the reported samples, prompting that the assay protocol should be improved to reduce this variability between supposedly identical samples. One way in which such improvements could likely be made would involve the collection of the media removed from the mammalian cells at the end of the incubation period. This fraction could also be analyzed for C.F.U content and then compared with the C.F.U counts of the adhered bacteria to determine the fraction of total bacteria that adhered to the epithelial cells. This would normalize the assay for different rates of bacterial proliferation, allowing the assay to focus on adhesion and not other measures of fitness so that the results would yield a more accurate picture of the effect of each displayed peptide solely on bacterial adhesion to the epithelium. The reproducibility and efficiency of the assay could also be improved with the use of a more accurate and easy to conduct

method for counting C.F.U. Instead of plating serial dilutions of cells, qPCR could be conducted with primers for *E. coli* 16S ribosomal RNA (Brosius et al., 1978), which would quantify the relative number of *E. coli* cells in each sample. This technique could also be used with both the removed media and the adherent cells, hopefully leading to more precise results.

Since increased adhesion could be used to modulate the localization of bacteria within the gut, future studies should use cell culture with epithelial cells from different regions of the gastrointestinal tract to determine whether the displayed peptides have different effects on adhesion in different sections of the gut. Such a finding is likely, given the different epithelial cell types for which the displayed peptides have shown affinity in the literature. Additionally, other cell conditions, such as injured or inflamed cells, should be investigated to determine whether certain peptides provide increased adherence to cells in these conditions, which could lead to the targeting of therapeutics.

# 6 Analysis of Displayed Trefoil Factor Family Peptide Biological Activity

Even with the successful confirmation of modified curli fiber expression, it is also possible that the entire appended peptide sequence could be displayed on the biofilm, but not in an active conformation, or its attachment to the biofilm could constrict its natural functionality. Therefore, further studies were conducted to assess the in vitro functionality and activity of the displayed trefoil factor family peptides. As stated above, the short peptides were assumed to be displayed on successfully secreted and assembled curli fibers, so further assays of their activity were not conducted. The assays conducted with the TFF-displaying curli fibers are outlined below.

## 6.1 Cyclooxygenase-2 Expression

Since the Trefoil Family Factor peptides are known to be secreted naturally in the human gastrointestinal tract and have an effect on the epithelia cells surrounding the gastrointestinal lumen (Taupin & Podolsky, 2003), a review of the literature was conducted to determine biological markers that are expressed by gastrointestinal epithelial cells in response to exposure to these peptides. The expression of one of these markers upon exposure to TFF-functionalized curli fibers but not upon exposure to wild type curli fibers would strongly suggest that the displayed TFF peptides are presented in an active conformation that is not inhibited by their attachment to the biofilm. Marker expression levels could also be measured in response to treatment with exogenous recombinant TFF peptides, but it should be noted that the level of TFF expression on the engineered curli fibers has yet to be determined, so the concentration of TFF peptide attached to the biofilm could not be correlated to

a recombinant peptide concentration, making direct comparisons between soluble recombinant peptides and curli bound peptides impossible.

Although the molecular mechanisms in response to the TFF peptides have not been fully elucidated,, a review of the literature reveals that cylooxygenase-2 (COX-2), also referred to as prostaglandin-endoperoxide synthase 2 (PTGS-2) in some studies, is expressed by human intestinal epithelial cells in response to TFF peptides (Tan et al., 2000; Rodrigues et al., 2001; Vandenbroucke et al., 2004). COX-2, one of the two COX isoforms, catalyzes the first two steps of the biosynthesis of prostaglandins G2 and H2 (Rouzer & Marnett, 2009), which are lipids known to play a role in the mediation of inflammation, pain, and cell proliferation (Marnett, 2009). Studies have shown that COX-2 inhibition reduced many of the cytoprotective effects due to TFF peptides, such as protection from reactive oxygen species-induced cell injury (Tan et al., 2002), so it is hypothesized that COX-2 plays a significant role in the therapeutic nature of the TFF peptides (Vandenbroucke et al., 2004). The physiological role of COX-2, however, is highly complex and yet to be fully understood, as COX-2 is also inhibited by nonsteroidal anti-inflammatory drugs (NSAIDs) (Vane, 1971), suggesting that COX-2 could also play a role in increased inflammation and pain (Marnett, 2009). For the purposes of this study, COX-2 will be used as a marker, and it's downstream physiological activity will not be considered in depth. For reference, the 3D structure of COX-2 can be seen in Figure 26.

COX-2 is also a good biomarker of TFF activity for this study because it not highly expressed in unstimulated cells and tissues (Tan et al., 2000; Herschman, 1996). Figure 27, from Tan et al., 2000, shows the Western blotting results for COX-2 expression in IEC-18 rat intestinal epithelial cells treated with 2.5 $\mu$M exogenous TFF3 and in negative control cells without TFF3. The expression of E-cadherin, the product of a housekeeping gene, was also shown for normalization. The difference

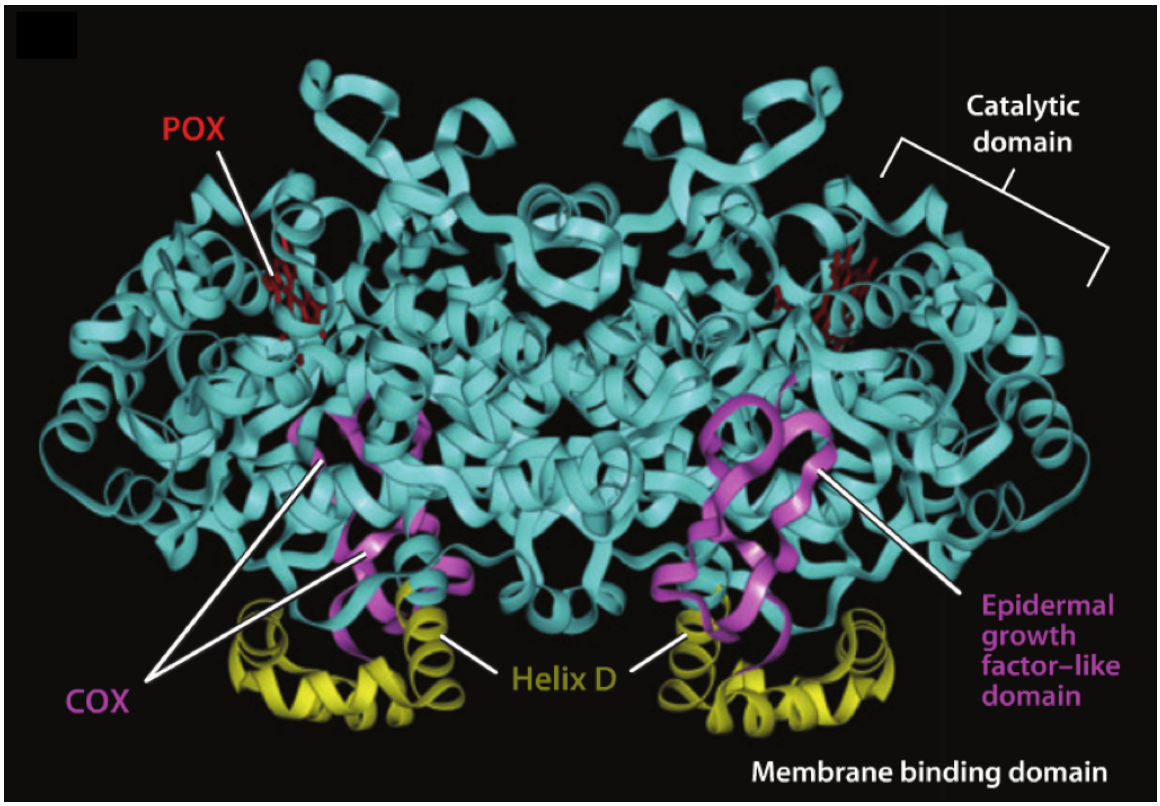


Figure 26: COX-2 structure, reproduced from Figure 5 of Marnett, 2009.

in band intensity is quite clear. Additionally, COX-2 has been used as a marker in a study investigating the therapeutic effects of recombinant TFF3 delivered by probiotic bacteria (Vandenbroucke et al., 2004), with clear results of increased cox-2 gene expression with TFF3 exposure during in vivo mouse studies.

Despite these advantages of using COX-2 as a marker for TFF peptide activity, it should also be noted that a recent study has implicated probiotic bacteria in the regulation of COX-2 (Otte et al., 2009). Therefore, careful comparisons between the effects of wild type and modified curli fibers will be needed. Additionally, this assay for COX-2 will be conducted with purified curli fibers sheared from their expressing bacterial cells to minimize the possible effects of living bacteria on the gene expression profile of the mammalian cells in cell culture to ensure that the displayed peptides

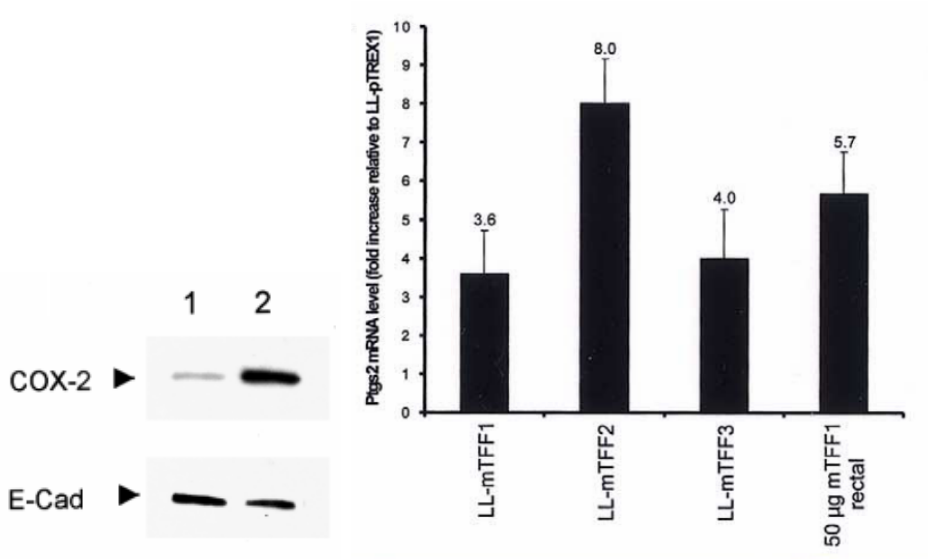


Figure 27: Previous studies have demonstrated increased COX-2 expression with the administration of rTFF3. Tan et al., 2000 on the left shows COX-2 expression in respone to 0 (Lane 1) or 2.5 $\mu$M rTFF3 (Lane 2). Vandenbroucke et al., 2004 on the right shows *csgA* mRNA levels from colon tissue samples collected after exposure to engineered probiotic bacteria secreting TFFs. Levels are relative to tissue exposed to bacteria not secreting TFFs.

are the source of observed differences.

## 6.2 Epithelial Reconstitution and Wound Healing

In addition to gene and protein expression, an indication of the curli-displayed TFF peptides effect on a more complex and therapeutic-related biological phenomenon was desired. As mentioned previously, the molecular mechanisms of TFF peptide therapeutic pathways are not fully understood and molecular markers, such as COX-2, may have multiple physiological roles that are complex and not well-characterized vis-à-vis therapeutic effects. Therefore, the wound-healing assay was chosen to assess these effects. This in vitro assay is designed to mimic cell migratory behavior during wound healing in vivo (Rodriguez et al., 2005) that has been well characterized and used extensively in the literature (Rosenberg et al., 1997).

Trefoil factor family peptides are well known to promote epithelial reconstitution and wound healing within the gut (Hoffmann, 2005; Guppy et al., 2012), and studies have specifically determined that TFF2 and TFF3 promote cell migration as a mechanism underlying such epithelial reconstitution (Dignass et al., 1994; Playford et al., 1995; Wong et al., 1999), making the wound healing assay an excellent TFF peptide activity and even therapeutic potential for the purposes of this study. Like the assay for COX-2 expression, the wound-healing assay has also been conducted for investigations of the effects of TFF3 expressed by probiotic bacteria (Vandenbroucke et al., 2004), with results indicating increased wound closure rates for CMT-93, a murine colorectal epithelial-derived cell line, cells when treated with murine TFF1, TFF2, and TFF3.

All of these biological activity assays will be conducted with the CaCo-2 cell line, a human epithelial colorectal adenocarcinoma-derived cell line frequently used for in vitro studies of the human gastrointestinal tract

## 6.3 Materials & Methods

### 6.3.1 Mammalian Cell Lines and Culture Conditions

CaCo-2 cells, were grown in culture according to previously described best practices (Natoli et al., 2012). Dulbecco's Modified Eagle Medium (DMEM) supplemented with 4.5 g/L D-glucose and L-glutamine but without sodium pyruvate (Gibco, Life Technologies, Carlsbad, CA, USA) was the standard base culture medium used, and future instances of DMEM in the text refer to this DMEM formulation. Cells were grown in DMEM supplemented with 15% fetal bovine serum (Gibco, Life Technologies, Carlsbad, CA, USA) and 1% pen/strep solution (5,000 units/mL of penicillin and 5000 $\mu$g/mL of streptomycin; Gibco, Life Technologies, Carlsbad, CA, USA) in

T75 tissue culture flasks (Corning Inc., Corning, NY, USA). Cells were incubated at 37°C with 5% CO2 . Cells were treated with trypsin-EDTA (Gibco, Life Technologies, Carlsbad, CA, USA) and passaged with a 1:20 dilution approximately every 72 hours. For certain assays, the concentrations of FBS and antibiotics were adjusted, as described in the following sections.

### 6.3.2 COX-2 Expression Assay

After passaging, 1 x $10^5$ CaCo-2 cells were added to each well of a 24-well tissue culture plate (Corning, Inc., Corning, NY, USA) in 500 $\mu$L DMEM supplemented with 15% FBS and 1% pen/strep solution and incubated at 37°C with 5% CO2 for 48 hours until confluent. The media was removed and replaced with 1% FBS-supplemented DMEM with 1% pen/strep, and then the cells were incubated at 37°C with 5% CO2 for an additional 24 hours, as previously described (Tan et al., 2000). The media was then replaced again (DMEM 1% FBS, 1% pen/strep) and the desired curli fibers (not monomers) were added to the appropriate wells, and the cells were incubated for 18 hours at 37°C with 5% $CO_2$. After this final incubation, cells were washed twice with ice cold DPBS, and then 100 $\mu$L of RIPA lysis and extraction buffer (G-Biosciences, St. Louis, MO, USA), supplemented with a protease inhibitor cocktail (cOmplete Tablets Mini, Roche, Basel, Switzerland), was added to each well. The cells were incubated with the lysis buffer on ice for 15 minutes before being scrapped from the well surface with a pipette and transferred to microcentrifuge tubes. The samples were centrifuged at 14,000g for 15 minutes to pellet the cell debris and the supernatants were collected for Western blotting.

Samples were prepared for SDS PAGE and the gels were run, stained, and analyzed. Western blot samples were prepared and Western blotting was conducted as described above in Section 4.4.4, except with the use of a rabbit polyclonal anti-

COX-2 primary antibody (Abcam, Cambridge, UK) and an anti-rabbit horseradish peroxidase-conjugated secondary antibody (Thermo Fischer Scientific). The primary COX-2 antibody was applied to the membrane at a 1:1000 dilution. A band representing COX-2 should fluoresce at approximately 69 kDa.

### 6.3.3 Wound Healing Assay

The wound healing assays were conducted essentially as previously described (Rosenberg et al., 1997; Rodriguez et al., 2005). After passaging, 1 x $10^5$ CaCo-2 cells were added to each well of a 24-well tissue culture plate (Corning, Inc., Corning, NY, USA) in 500 $\mu$L DMEM supplemented with 15% FBS and 1% pen/strep solution and incubated at 37°C with 5% $CO_2$ for 48 hours until confluent. The media was removed and replaced with 1% FBS-supplemented DMEM with 1% pen/strep, and then the cells were incubated at 37°C with 5% $CO_2$ for an additional 24 hours. A p10 pipette was then used to scrape a thin linear "wound" in the confluent monolayer. The cells were washed twice in PBS to remove all non-adherent cells, 500 $\mu$L fresh 1% FBS, 1% pen/strep DMEM media was added to each well, and the desired peptides or curli-fusion peptides were added to the appropriate wells. The plate was returned to the incubator at 37°C with 5% $CO_2$. At given time points, images were taken at 4x magnification using an Evos Cell Imaging System microscope (Life Technologies) to record the wound healing progress. The "wound" areas in each image, which are gray scale, were manually identified and colored red in Photoshop (Adobe Systems, Inc., San Jose, CA, USA). A custom MATLAB (MathWorks, Natick, MA, USA) script developed by the author was used to determine the size of all the wounds. A representative example of this image processing procedure for one wound can be a found in Figure 28.

The wound-healing assay was also conducted with live bacterial cells expressing

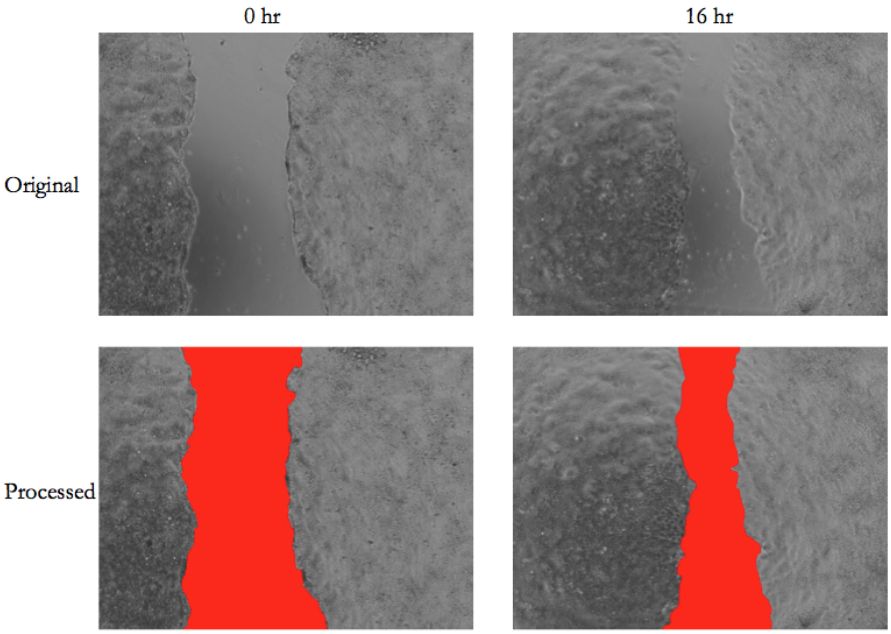


Figure 28: Wound healing assay image processing

engineered curli fibers. For these assays, CaCo-2 cells were grown to confluent monolayers and wounded, as described above, but instead of curli or peptides, transformed bacterial cells expressing the different constructs were added to the monolayers, 1 X $10^7$ per well. These bacterial cells had been inoculated and grown to mid-log phase in carbenicillin supplemented LB, transferred to carbenicillin supplemented YESCA media, induced with 0.3 mM IPTG, and incubated overnight at 25°C with shaking. When these bacteria were added to the wounded monolayers, the tissue culture growth medium was changed to DMEM 1% FBS with no pen/strep but supplemented with 0.3 mM IPTG so that the bacteria could survive and continue to express curli fibers.

### 6.3.4 Wound Healing Assay Device

After initial trials of the wound-healing assay, it was noted that the wounds inflicted by the pipette tips were non-uniform and differed widely in width and morphology, likely contributing to the large error observed in these trials. To reduce such discrepancies in "wounds", it was hypothesized that uniform pieces of a biocompatible material in the shape of a thin rectangle could be placed on the bottom of the tissue culture well before cells were added to prevent cells from adhering to the well surface underneath the material. The cells should continue to proliferate and form confluent monolayers on the rest of the well, and then this piece of material could be removed to generate the "wound". Since the device would alter the properties of the tissue culture plastic underneath it, the cells should still be able to migrate back across the surface to reconstitute the wounded region.

Such a device would be on the scale of 10 $mm^3$, due to the small size of the wells in a 24 well tissue culture plate (2 $cm^2$ well bottom surface area, 18 mm well depth), and at least 24 would need to be manufactured for a full plate assay, so 3D printing was chosen as the best method for prototyping and manufacturing. The device was designed in SolidWorks 3D CAD Design Software (Dassault Systèmes SolidWorks Corp., Waltham, MA, USA) and prepared for 3D printing with the addition of temporary support structures using PreForm Software (Formlabs, Inc., Somerville, MA, USA). The devices were printed on a Form1 3D printer (Formlabs, Inc., Somerville, MA, USA) using FormLabs Clear Photoactive Resin (FormLabs Inc., Somerville, MA, USA), which is a proprietary mixture of methacrylic acid esters, acrylic acid esters, and photoinitiator compound. After printing, the devices were soaked in 90% isopropyl alcohol for 30 minutes to remove any excess resin and weaken temporary support structures. The remaining temporary supports were then manually removed

with wire clippers and support marks were gently sanded. Before use in tissue culture conditions, the devices were autoclaved on a gravity cycle at 121°C with a 15 minute sterilization time and then a 20 minute drying time. The devices were placed into the tissue culture plate wells using tweezers and oriented uniformly with the wounding surface along either the longitudinal or latitudinal axis of the wells. CaCo-2 containing media was added to each well on both sides of the wounding surface. After monolayer complacency was reached, the devices were carefully removed with tweezers, being careful to minimize any rotational or horizontal translational movement that might interfere with the monolayers on either side of the wounding surface.

The design had be modified and improved to ensure that it did not interfere with the ability for the growing cells to engage in gas exchange with the incubator environment. Early versions of the device made contact with the plate lid, preventing such gas exchange from occurring. Additionally, portions of the device had to be thickened to ensure that they could withstand the harsh conditions of the autoclave. The iteration of designs of the device can be seen in Figure 29.

Sara Hamel, the Biological and Environmental Laboratory Manager for the Harvard SEAS Undergraduate Teaching Laboratories, was incredibly helpful during the 3D printing process, and generously allowed the author to use the 3D printing equipment in the SEAS Undergraduate Teaching Laboratories.

### 6.3.5 Data Analysis

Western blot membrane images were analyzed with ImageJ (National Institutes of Health, Bethesda, MD, USA; Schneider et al., 2012) to determine band intensities. All plots were generated using MATLAB.

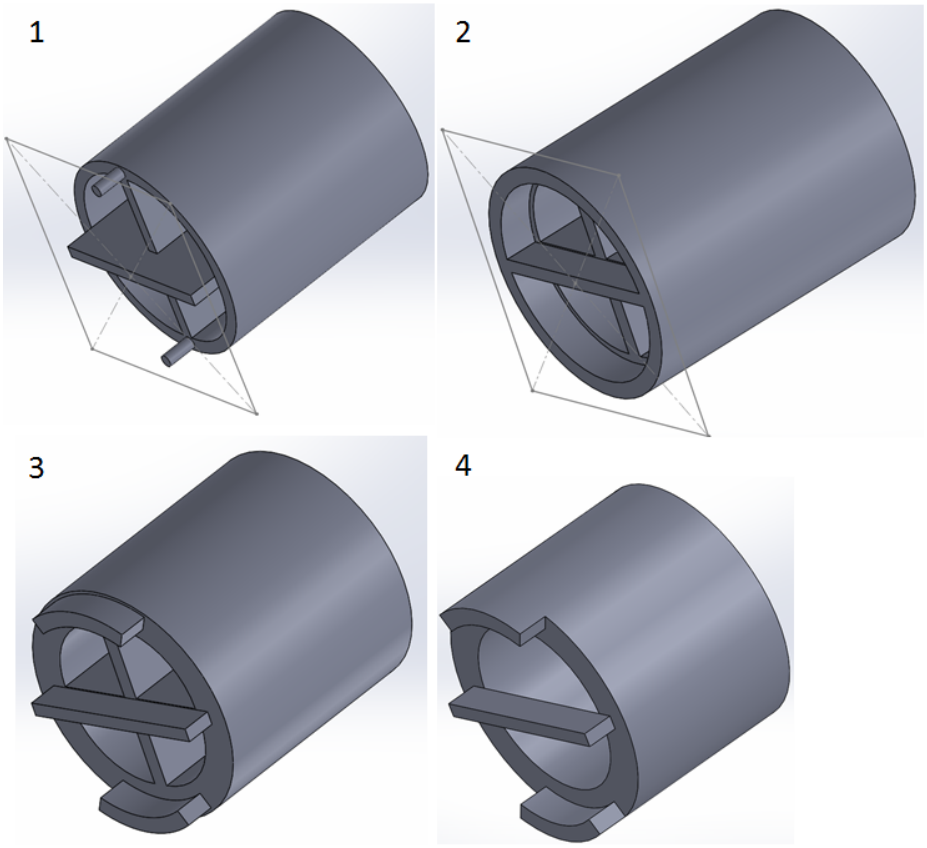


Figure 29: Design iterations of the wound healing assay device.

## 6.4 Results and Discussion

### 6.4.1 COX-2 Expression

Due to time constraints and the previously discussed difficulties with curli fiber purification and monomerization, conclusive results were not obtained for the COX-2 expression assays. Good progress concerning assay design and optimization, however, was achieved and the results presented here represent an excellent starting point for ongoing work in the Joshi Lab with these assays.

Initial assays confirmed previous literature, and demonstrated that the application of exogenous TFF3 does indeed enhance the expression of COX-2 in CaCo-2 human

intestinal epithelial cells, as seen in Figure 30 .

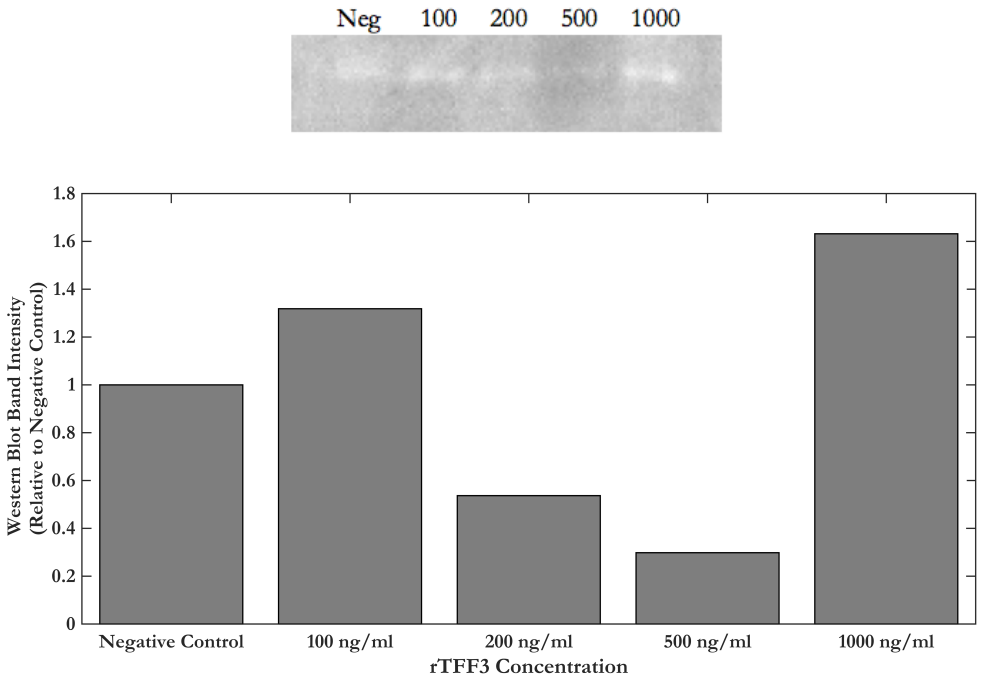


Figure 30: Western blotting for COX-2 expression in response to the application of exogenous recombinant TFF3. The top image shows the bands at 69 kDa, the predicted molecular weight of COX-2, with the concentration of rTFF3 in ng/ml listed above each lane. The plot shows the intensities of these bands relative to the negative control without any rTFF3. $n = 1$

Results with the application of purified curli and engineered curli fibers were not as conclusive, however, as can be seen in Figure 31. Issues with reproducibility can likely be attributed to problems with resuspending the semi-purified curli samples. Many clumps formed that could not be resuspended, even with aggressive shaking and vortexing. As a result, when samples were collected for application to CaCo-2 cell culture, the amount of TFF-modified curli obtained was not necessarily uniform, depending upon whether or not one of these clumps was present in the collected sample. Future work will need to address this issue, possibly having to employ a different purification protocol. Additionally, the presence of non-uniform spots seen in

some of the Western blot bands indicates that COX-2 may not have been successfully removed from the rest of cellular components, so future assays will need to employ the use of a stronger lysis buffer to ensure that COX-2 is more effectively separated from the cellular debris. It should also be noted that the curli fibers applied here were monomerized, but CsgA-TFF monomers might yield better results. The use of monomers, however, would not as accurately represent the *in vivo* application of biofilms that this study is trying to replicate *in vitro*.

### 6.4.2 Wound Healing Assays

Like the COX-2 expression assays, time constraints and difficulties with curli purification limited the collection of data for the wound healing assay, but substantial progress has been made that will improve future wound healing assays with modified curli fibers. Initial assays confirmed previous work indicating that the application of exogenous TFF3 does in fact improve the rate of wound closure in CaCo-2 cells, as shown in Figure 32, with statistically significant increases in wound closure rates for 200 ng/ml and 500 ng/ml rTFF3 as compared with the negative control (see Table 11 for p-values). There were, however, some significant inconsistencies between samples under the same conditions. It was observed that many of the initial wounds created with a pipette tip were not uniform and had varying morphologies and widths at the 0 hr time point, so it was hypothesized that a more uniform wounding procedure would likely lead to more consistent final results. Therefore, a so-called wound healing assay device was designed to create uniform wounds in the CaCo-2 monolayers. The development of this device will greatly improve the reproducibility and ease of execution of these assays in the Joshi Lab going forward.

The wound healing assay was also conducted once with live bacterial cells expressing the engineered curli fibers, but co-culture with the live bacterial cells and

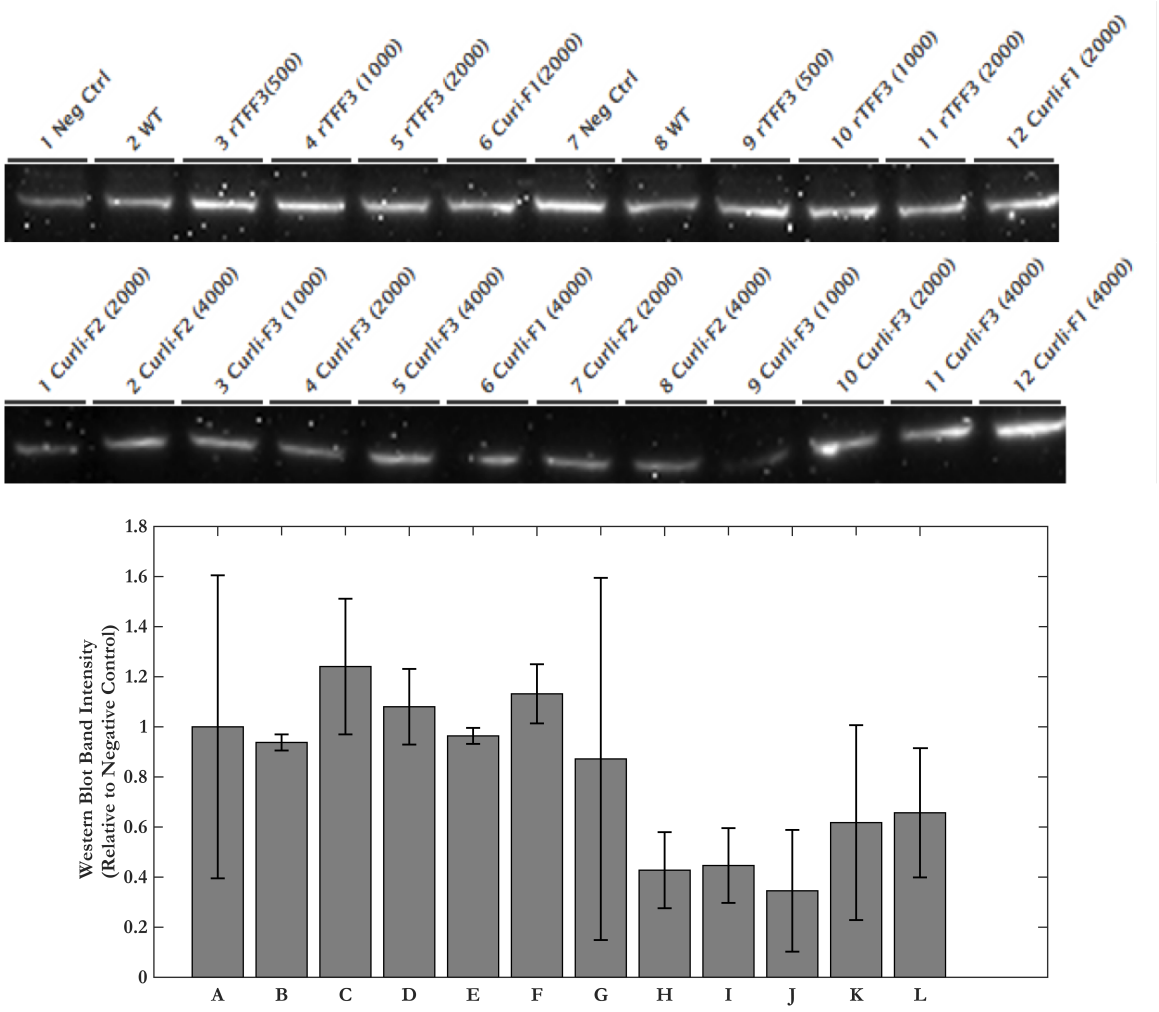


Figure 31: Western blotting for COX-2 expression in response to the application of exogenous recombinant TFF3 and modified curli fibers.The top image shows the bands at 69 kDa, the predicted molecular weight of COX-2, with the substance added listed above each lane. The concentration of each solution in ng/ml is listed in parentheses. The plot shows the intensities of these bands relative to the negative control. The x axis is coded as follows: (A) Negative Control, (B) Wild Type Curli, (C) 500 ng/ml rTFF3, (D) 1000 ng/ml rTFF3, (E) 2000 ng/ml rTTTF, (F) 2000 ng/ml CsgA-48-TFF1, (G) 4000 ng/ml CsgA-48-TFF1, (H) 2000 ng/ml CsgA-24-TFF2, (I) 4000 ng/ml CsgA-24-TFF2, (J) 1000 ng/ml CsgA-24-TFF3, (K) 2000 ng/ml CsgA-24-TFF3, (L) 4000 ng/ml CsgA-24-TFF3. For all conditions, $n = 2$; error bars represent standard deviations

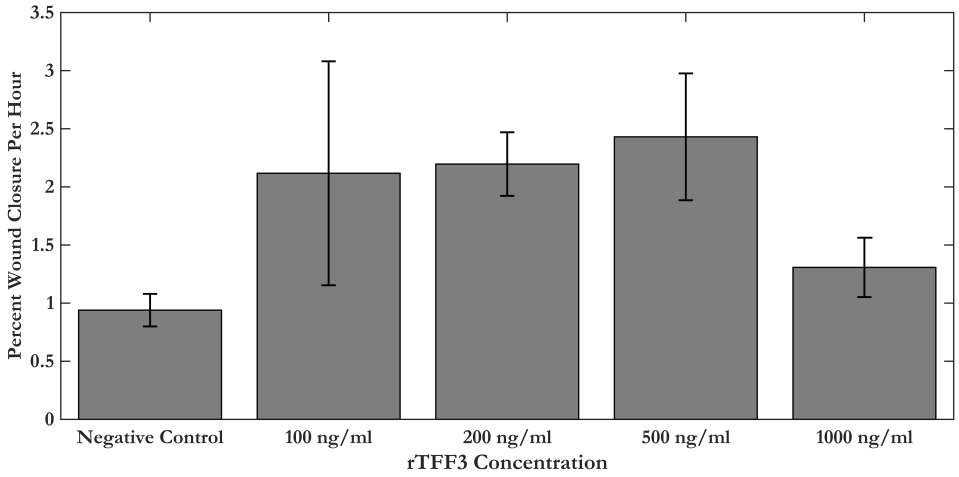


Figure 32: Wound healing assay conducted with the application of exogenous recombinant TFF3. The plot shows the rate of wound closure as the percentage of original wound width closed per hour . $n = 6$; error bars represent standard error.

| rTFF3 Concentration | Comparison to Negative Control |
|---|---|
| 100 ng/ml | $p = 0.0821$ |
| 200 ng/ml | $p < 0.001$ |
| 500 ng/ml | $p = 0.002$ |
| 1000 ng/ml | $p = 0.215$ |

Table 11: Statistical significance of results for the rTFF3 wound healing assay. $p < 0.005$ is considered significant.

mammalian cells proved problematic due to the significant competition for the limited resources of the growth media in each well. As a result, the CaCo-2 cells, which as an immortalized cell line are highly sensitive, began to sicken and die as the bacterial cells proliferated and consumed the nutrients in the media, leading to very slow wound closure rates and significant inconsistencies between trials, as can be seen in Figure 33. It was hypothesized that the use of a bacteriostatic inhibitor might alleviate some of these issues by preventing the bacteria from proliferating, but a review of the literature did not reveal a suitable candidate inhibitor that would not likely

affect the CaCo-2 cells.

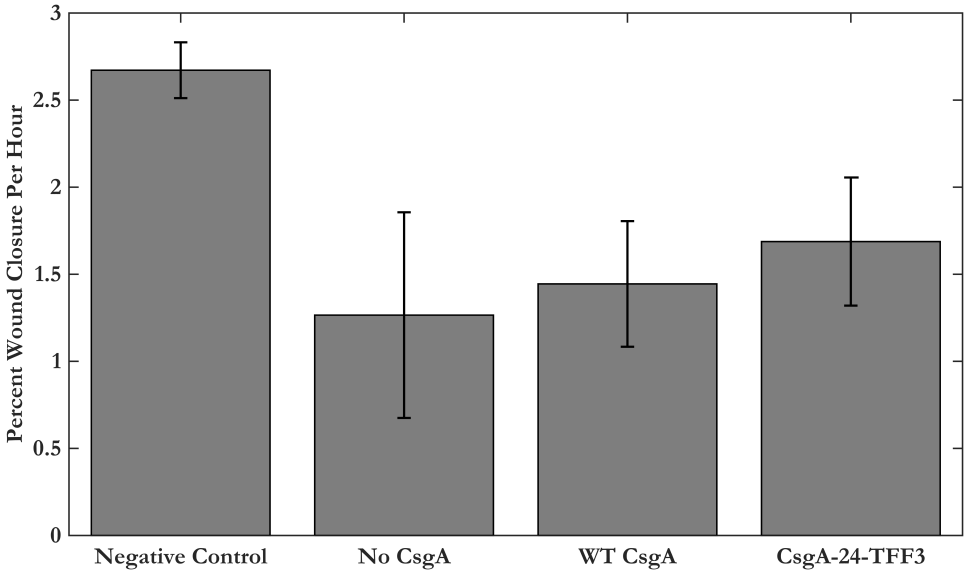


Figure 33: Wound healing assay conducted with live *E. coli* expressing curli fibers. The plot shows the rate of wound closure as the percentage of original wound width closed per hour. $n = 3$; error bars represent standard deviation.

After completing the production of the wound healing devices and the purification of the engineered curli fibers, there was not enough time to conduct another wound healing assay, but the work presented here represents a strong foundation for the future use of the wound healing assay with TFF-modified curli fibers in the Joshi Lab.

## 6.5 Future Work

As is clear from the above discussion of results, further experiments are required to improve upon the initial results of the peptide activity assays. Addressing the curli fiber purification and resuspension issues will likely improve the reproducibility of results from the COX-2 expression assay, as this will allow for a more uniform

application of curli fibers across all of the mammalian cell samples. Improved cell lysis will also likely lead to better COX-2 assay results by ensuring that all of the expressed COX-2 is released into the cell lysate for blotting. Improved curli purification and resuspension, combined with the application of the wound healing device, will likely lead to consistent and informative wound healing assay results.

In addition to the assays already conducted, qPCR could be conducted to measure the expression of the *cox-2* gene. It seems to be almost standard practice in the field when studying the activation of a gene and subsequent protein expression to report both qPCR data, which is indicative of transcription of the gene in question, and western blotting data, which is indicative of proper protein expression. qPRC could also easily be used to investigate the expression of other TFF activity markers reported in the literature, such as *cldn-1* and *cldn-2*(zum Buschenfelde, et al., 2006), especially if COX-2 expression does not change in response to the appliation of TFF-modified curli fibers. qPRC primers have already been designed for *cox-2*, *cldn-1* , *cldn-2*, and *gapdh*, a housekeeping gene commonly used to normalize qPCR measurements across samples.

# 7 Conclusions and Future Work

The work presented here provides a strong foundation for the development of the desired biofilm-based platform for controling the localized adhesion and therapeutic effects of the expressing bacteria within the mammalian gastrointestinal tract. A library of CsgA-fusion genetic constructs was successfully created and *E. coli* transformed with at least one of the CsgA-fusion constructs for each desired functional peptide could secrete curli fibers at levels similar to that of wild type CsgA. More thorough analysis of molecular weight via SDS-PAGE confirmed that the CsgA-TFF monomers were the correct size, and western blotting identified the TFF2 and TFF3 peptides displayed on curli fibers. Adhesion assays determined that the curli-displayed T18 peptide significantly increases the ahesion of expressing bacteria to intestinal epithelial cells, and future improvements to the assay design will likely reveal more peptides with increased adhesion. The optimization of the peptide display and activity assays begun here will be continued, and upon their successful completion, the platform will be ready to move toward translation.

For translation, the platform will need to be implemented with a probiotic strain of *E. coli* that could survive in the competitive environment of the gastrointestional tract, which the lab strains invesetigated in this study could not. One such probiotic strain that has the cellular machinery necessary for curli secretion and assembly is the *E. coli* Nissle 1917 (EcN) strain. Work has already been completed in the Joshi Lab to create a *csgA* knockout strain of Nissle 1917, that could then be transformed with the engineered constructs. To remove the need for IPTG induction, the constructs could be genomically incorporated using CRISPR-Cas technology, placing the constructs under the native curli biogenesis regulation.

After successful incorporation with Nissle, the platform could be tested in more

realistic *in vitro* environments, such as the human Gut-on-a-Chip model (Kim et al., 2012), which would allow for longer adhesion studies, given the flow of fresh media through the device, and provide data on more inflammation markers to assess the activity of the TFF peptides. *In vivo* mouse studies could then be conducted to investigate adhesion in different regions of the gastrointestinal tract and to investigate the therapeutic effects DSS-induced acute colitis model mice.

Overall, a foundation has been laid for the development of a biofilm-based therapeutic platform that has the long-term potential to improve treatment outcomes for millions of people suffering from inflammatory bowel diseases.

# References

In: ().

Aamann, L, E Vestergaard, and H Gronbaek. "Trefoil factors in inflammatory bowel disease." In: *World journal of gastroenterology : WJG* 20.12 (2014), pp. 3223–3230.

Barnhart, M and M Chapman. "Curli biogenesis and function". In: *Annu. Rev. Microbiol.* 60 (2006), pp. 131–147.

Brosius, J, ML Palmer, and PJ Kennedy. "Complete nucleotide sequence of a 16S ribosomal RNA gene from Escherichia coli". In: (1978). DOI: 10.1073/pnas.75.10.4801. URL: http://dx.doi.org/10.1073/pnas.75.10.4801.

Chapman, Matthew R et al. "Role of Escherichia coli curli operons in directing amyloid fiber formation." In: *Science* 295.5556 (2002), pp. 851–855.

Collinson, S et al. "Thin, aggregative fimbriae mediate binding of Salmonella enteritidis to fibronection." In: *Journal of Bacteriology* 175 (1993), pp. 12–18.

Collinson, SK, L Emody, and KH Muller. "Purification and characterization of thin, aggregative fimbriae from Salmonella enteritidis." In: *Journal of Bacteriology* 173 (1991), pp. 12–18.

Costantini, T et al. "Targeting the gut barrier: identification of a homing peptide sequence for delivery into the injured intestinal epithelial cell." In: *Surgery* 146.2 (2009), pp. 206–212.

Dignass, A, Lynch-Devaney, K, and H Kindon. "Trefoil peptides promote epithelial migration through a transforming growth factor beta-independent pathway." In: (1994).

Evans, M et al. "The Bacterial Curli System Possesses a Potent and Selective Inhibitor of Amyloid Formation". In: *Melecular Cell* 57 (2015), pp. 445–455.

Fakhoury, M et al. “Inflammatory bowel disease: clinical aspects and treatments”. In: *Journal of Inflammation Research* 2014.7 (2014), pp. 113–120.

Gerven, N et al. “Secretion and functional display of fusion proteins through the curli biogenesis pathway”. In: *Molecular Microbiology* 91.5 (2014), pp. 1022–1035.

Gibson, Daniel G et al. “Enzymatic assembly of DNA molecules up to several hundred kilobases.” In: *Nature methods* 6.5 (2009), pp. 343–345.

Goyal, P et al. “Structural and mechanistic insights into the bacterial amyloid secretion channel CsgG”. In: *Nature* 516 (2014), pp. 250–256.

Guppy, Naomi J et al. “Trefoil factor family peptides in normal and diseased human pancreas”. In: *Pancreas* 41.6 (2012), pp. 888–896.

H, LeVine, “Quantification of beta-sheet amyloid fibril structures with thioflavin T.” In: *Methods in Enzymology* 309 (1999), pp. 274–284.

Hammar, M et al. “Expression of two csg operons is required for production of fibronectin- and congo red-binding curli polymers in Escherichia coli K12”. In: ().

Higgins, LM et al. “In vivo phage display to identify M cell-targeting ligands”. In: *Pharmaceutical Research* 21.4 (2004).

Hoffmann, W. “Trefoil factor family (TFF) peptides and chemokine receptors: a promising relationship”. In: *Journal of Medicinal Chemistry* 52 (2009), pp. 6505–6510.

— “Trefoil factor family (TFF) peptides: regulators of mucosal regeneration and repair, and more”. In: *Peptides* 25.5 (2005).

Horton, RM et al. “Engineering hybrid genes without the use of restriction enzymes: gene splicing by overlap extension”. In: *Gene* 77 (1989), pp. 61–68.

Hsiung, PL et al. “Detection of colonic dysplasia in vivo using a targeted heptapeptide and confocal microendoscopy”. In: *Nature Medicine* (2008).

Kim, H and D Ingber. "Gut-on-a-Chip microenvironment induces human intestinal cells to undergo villus differentiation". In: *Integrative Biology* 5.9 (2013), pp. 1130–1140.

Klunk, WE, RF Jacob, and RP Mason. "Quantifying amyloid by congo red spectral shift assay." In: *Methods in Enzymology* 309 (1999), pp. 285–305.

Koli, P et al. "Conversion of Commensal Escherichia coli K-12 to an Invasive Form via Expression of a Mutant Histone-Like Protein". In: *mBio* 2.5 (2011), e00182–e00111.

Lee, TS et al. "BglBrick vectors and datasheets: a synthetic biology platform for gene expression". In: *Journal of Biological Engineering* 5.12 (2011).

Letourneau, J, C Levesque, and F Berthiaume. "In vitro assay of bacterial adhesion onto mammalian epithelial cells". In: (2011).

Marnett, Lawrence J. "The COXIB experience: a look in the rearview mirror." In: *Annual review of pharmacology and toxicology* 49 (2008), pp. 265–290.

Michelitsch, MD and JS Weissman. "A census of glutamine/asparagine-rich regions: implications for their conserved function and the prediction of novel prions." In: *Proceedings of the National Academy of Sciences of the United States of America* 97.22 (2000), pp. 11910–11915.

Natoli, Manuela et al. "Good Caco-2 cell culture practices." In: *Toxicology in vitro : an international journal published in association with BIBRA* 26.8 (2012), pp. 1243–1246.

Nguyen, Peter Q et al. "Programmable biofilm-based materials from engineered curli nanofibres." In: *Nature Communications* 5.5945 (2014).

"Nucleator-dependent intercellular assembly of adhesive curli organelles in Escherichia coli." In: *Proc. Natl. Acad. Sci. USA* 93 (1996), pp. 6562–6566.

Otte, J and R Mahjurian-Namari. “Probiotics regulate the expression of COX-2 in intestinal epithelial cells.” In: *Nutrition and cancer* 61.1 (2009), pp. 103–113.

Perutz, MF et al. “Amyloid fibers are water-filled nanotubes.” In: *Proceedings of the National Academy of Sciences of the United States of America* 99.8 (2002), pp. 5591–5595.

Playford, R et al. “Human Spasmolytic Polypeptide is a Cytoprotective Agent That Stimulates Cell Migration.” In: ().

Podolsky, DK. “Healing the epithelium: solving the problem from two sides”. In: *Journal of Gastroenterology* 32 (1997), pp. 122–126.

Poulsom, R, R Chinery, and C Sarraf. “Trefoil peptide gene expression in small intestinal Crohn’s disease and dietary adaptation.” In: *Journal of Clinial Gastroenterology* 17 (1993).

Puttamreddy, S and Minion F. “Linkage between cellular adherence and biofilm formation in Escherichia coliO157:H7 EDL933”. In: *FEMS Microbiology Letters* 315.1 (2011), pp. 46–53.

Robinson, Lloyd S et al. “Secretion of curli fibre subunits is mediated by the outer membrane-localized CsgG protein.” In: *Molecular microbiology* 59.3 (2006), pp. 870–881.

Rodrigues, S et al. “Activation of cellular invasion by trefoil peptides and src is mediated by cyclooxygenase- and thromboxane A2 receptor-dependent signaling pathways”. In: *The FASEB Journal* 15.9 (2001), pp. 1517–1528.

R{” g, m i et al. “Occurrence and regulation of the multicellular morphotype in Salmonella serovars important in human disease”. In: *Int. J. Med. Microbiol.* 293 (2003), pp. 273–285.

Rosenberg, IM, k G{” ¿, “Epithelial cell kinase-B61: an autocrine loop modulating intestinal epithelial migration and barrier function”. In: (1997).

Rouzer, Carol A and Lawrence J Marnett. "Cyclooxygenases: structural and functional insights." In: *Journal of lipid research* 50 Suppl (2009), S29–S34.

Schneider, CA, WS Rasband, and KW Eliceiri. "NIH Image to ImageJ: 25 years of image analysis". In: *Nature Methods* 9.7 (2012), pp. 671–675.

Simm, Roger et al. "GGDEF and EAL domains inversely regulate cyclic di-GMP levels and transition from sessility to motility." In: *Molecular microbiology* 53.4 (2004), pp. 1123–1134.

Smith, Jeffrey F et al. "Characterization of the nanoscale properties of individual amyloid fibrils." In: *Proceedings of the National Academy of Sciences of the United States of America* 103.43 (2006), pp. 15806–15811.

Steidler, L. "Genetically engineered probiotics". In: *Best Practice & Research Clinical Gastroenterology* 17.5 (2003), pp. 861–876.

Steidler, L and P Rottiers. "Therapeutic drug delivery by genetically modified Lactococcus lactis". In: *Annals of the New York Academy of Sciences* 1072 (2006), pp. 176–186.

Sunde, M and C Blake. "The structure of amyloid fibrils by electron microscopy and X-ray diffraction". In: *Advanced Protein Chemistry* 50 (1997), pp. 123–159.

Tan, X, Y Chen, and Q Liu. "Prostanoids mediate the protective effect of trefoil factor 3 in oxidant-induced intestinal epithelial cell injury: role of cyclooxygenase-2." In: *Journal of Cell Science* 113 (2000), pp. 2149–2155.

Taupin, D and DK Podolsky. "Trefoil factors: initiators of mucosal healing". In: *Nature Reviews Molecular Cell Biology* 4 (2003), pp. 721–734.

Taylor, JD et al. "Atomic resolution insights into curli fiber biogenesis". In: *Structure* 19 (2011), pp. 1307–1316.

Thim, L. "Trefoil peptides: from structure to function." In: *Cellular and molecular life sciences : CMLS* 53.11-12 (1997), pp. 888–903.

Vandenbroucke, K et al. “Active delivery of trefoil factors by genetically modified Lactococcus lactis prevents and heals acute colitis in mice”. In: *Gastroenterology* 127.2 (2004), pp. 502–513.

Vane, JR. “Inhibition of prostaglandin synthesis as a mechanism of action for aspirin-like drugs.” In: *Nature: New biology* 231.25 (1971), pp. 232–235.

Wong, WM, R Poulsom, and NA Wright. “Trefoil peptides.” In: *Gut* 44.6 (1999), pp. 890–895.

Wright, Nicholas A et al. “Epidermal growth factor (EGF/URO) induces expression of regulatory peptides in damaged human gastrointestinal tissues”. In: *The Journal of Pathology* 162.4 (1990), pp. 279–284.

Wu, Chun, Justin Scott, and Joan-Emma E Shea. “Binding of Congo red to amyloid protofibrils of the Alzheimer A(9-40) peptide probed by molecular dynamics simulations.” In: *Biophysical journal* 103.3 (2012), pp. 550–557.

Zhang, Y et al. “Panning and identification of a colon tumor binding peptide from a phage display peptide library”. In: *Journal of Biomolecular Screening* 12.3 (2007), pp. 429–435.

Zhou, Y et al. “Experimental manipulation of the microbial functional amyloid called curli”. In: (2013).

Zogaj, X et al. “The multicellular morphotypes of Salmonella typhimurium and Escherichia coli produce cellulose as the second component of the extracellular matrix.” In: *Molecular microbiology* 39.6 (2001), pp. 1452–1463.

# Appendix A Nucleic Acid Sequences of CsgA Construct Components

Wild Type CsgA:

ATGAAACTTTTAAAAGTAGCAGCAATTGCAGCAATCGTATTCTCCGGTAG
CGCTCTGGCAGGTGTTGTTCCTCAGTACGGCGGCGGCGGTAACCACGGTG
GTGGCGGTAATAATAGCGGCCCAAATTCTGAGCTGAACATTTACCAGTAC
GGTGGCGGTAACTCTGCACTTGCTCTGCAAACTGATGCCCGTAACTCTGA
CTTGACTATTACCCAGCATGGCGGCGGTAATGGTGCAGATGTTGGTCAGG
GCTCAGATGACAGCTCAATCGATCTGACCCAACGTGGCTTCGGTAACAGC
GCTACTCTTGATCAGTGGAACGGCAAAAATTCTGAAATGACGGTTAAACA
GTTCGGTGGTGGCAACGGTGCTGCAGTTGACCAGACTGCATCTAACTCCT
CCGTCAACGTGACTCAGGTTGGCTTTGGTAACAACGCGACCGCTCATCAG
TAC

F12 Linker

GGTGGTGGTTCTGGCGGTGGCTCCGGTGGTGGCTCT

F24 Linker:

GGCGGCGGTTCTGGTGGCGGCTCTGGTGGTGGCTCTGGCGGCGGATCTGG
TGGTGGTTCTGGCGGCGGTTCC

F48 Linker:

GGTGGTGGTAGTGGTGGCGGCAGTGGTGGCGGTAGCGGCGGTGGCTCCGG
TGGCGGTTCTGGCGGCGGTTCTGGTGGTGGTTCTGGCGGTGGCTCAGGTG
GGGGTTCCGGCGGCGGTAGCGGCGGTGGATCTGGCGGCGGCTCT

TFF1:

GAAGCGCAGACCGAAACCTGCACCGTGGCGCCGCGCGAACGCCAGAACTG
CGGCTTTCCGGGCGTGACCCCGAGCCAGTGCGCGAACAAAGGCTGCTGCT

TTGATGATACCGTGCGCGGCGTGCCGTGGTGCTTTTATCCGAACACCATT

GATGTGCCGCCGGAAGAAGAATGCGAATTT

TFF2:

GAAAAACCGAGCCCGTGCCAGTGCAGCCGCCTGAGCCCGCATAACCGCAC

CAACTGCGGCTTTCCGGGCATTACCAGCGATCAGTGCTTTGATAACGGCT

GCTGCTTTGATAGCAGCGTGACCGGCGTGCCGTGGTGCTTTCATCCGCTG

CCGAAACAGGAAAGCGATCAGTGCGTGATGGAAGTGAGCGATCGCCGCAA

CTGCGGCTATCCGGGCATTAGCCCGGAAGAATGCGCGAGCCGCAAATGCT

GCTTTAGCAACTTTATTTTTGAAGTGCCGTGGTGCTTTTTTCCGAAAAGC

GTGGAAGATTGCCATTAT

TFF3:

GAAGAATATGTGGGCCTGAGCGCGAACCAGTGCGCGGTGCCGGCGAAAGA

TCGCGTGGATTGCGGCTATCCGCATGTGACCCCGAAAGAATGCAACAACC

GCGGCTGCTGCTTTGATAGCCGCATTCCGGGCGTGCCGTGGTGCTTTAAA

CCGCTGCAGGAAGCGGAATGCACCTTT